UNCLASSIFIED

AD **299 356**

Reproduced
by the

ARMED SERVICES TECHNICAL INFORMATION AGENCY
ARLINGTON HALL STATION
ARLINGTON 12, VIRGINIA
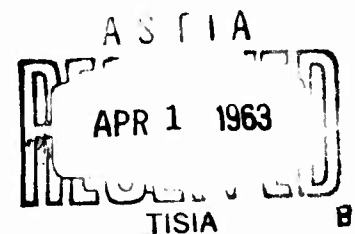
STAGNATION AND WAKE FLOWS
NORMAL TO A FLAT SURFACE

by

Ernst W. Schwiderski and Hans J. Lugt
Computation and Analysis Laboratory

U. S. NAVAL WEAPONS LABORATORY
DAHLGREN, VIRGINIA

Date: FEBRUARY 1963

U. S. Naval Weapons Laboratory
Dahlgren, Virginia

Stagnation and Wake Flows

Normal to a Flat Surface

by

Ernst W. Schwiderski and Hans J. Lugt
Computation and Analysis Laboratory

NWL REPORT NO. 1840

Task Assignment
NO. R360FR103/2101/R01101001

February 1963

TABLE OF CONTENTS

ABSTRACT

Complete numerical results of axisymmetric and plane stagnation
and wake flows, which are produced by homogeneous motions with finite
initial velocities normal to a flat surface, are presented for a
variety of Reynolds numbers. The results have been obtained on the
basis of an extension of Prandtl's boundary layer theory. Charac-
teristic flow properties are pointed out and discussed. Critical
Reynolds numbers for nonexistent laminar attached flows are
computed.

FOREWORD

This work was sponsored by the Naval Weapons Laboratory Foundational Research Program. It was performed in the Computation and Analysis Laboratory as part of the Meteorological and Oceanographical project (R360FR103/2101/R01101001).

The authors wish to extend their thanks to Dr. C. J. Cohen for many critical and stimulating discussions.

The date of completion was 11 February 1963.

Approved for Release:

/s/ R. H. LYDDANE
Technical Director

1. Introduction

Axisymmetric and plane stagnation and wake flows "normal" to a flat surface have been investigated in [4] on the basis of the extended boundary layer theory which was introduced in [3]. In contrast to the classical stagnation flows "past" a flat surface, which are produced by nonhomogeneous motions of infinite initial velocities (see [1, 2]), the new stagnation flows are generated by homogeneous motions of finite initial velocities (see Fig. 1). While the classical stagnation flows represent significant models for real flows past blunt bodies, the new flows are of interest in the design of piston machines.

In [4] the Navier-Stokes equations have been reduced to a single ordinary differential equation which has been solved by the Runge-Kutta method. Complete numerical results of axisymmetric and plane stagnation and wake flows are displayed in the present paper for a selected variety of Reynolds numbers. Characteristic properties of these flows are pointed out and discussed.

1

2. The Reduced Navier-Stokes Equations

In a plane or axisymmetric stagnation or wake flow normal to a flat solid surface let (r, z) be an orthogonal coordinate system in which z = 0 denotes the solid surface and r = 0 the axis of symmetry of the flow (see [4] and Fig. 1). The corresponding velocity (u, w) of the flow with the variable pressure p and the constant density and kinematic viscosity ρ and υ is determined by the Navier-Stokes equations

$$uu_r + wu_z = - \frac{1}{\rho} p_r + \upsilon \left[u_{rr} + n\left(\frac{u}{r}\right)_r + u_{zz} \right] \tag{1}$$

$$uw_r + ww_z = - \frac{1}{\rho} p_z + \upsilon \left[w_{rr} + \frac{n}{r} w_r + w_{zz} \right] \tag{2}$$

$$u_r + \frac{n}{r}u + w_z = 0 \tag{3}$$

The unifying parameter n assumes the value n = 0 for plane flows and n = 1 for axisymmetric motions.

The stagnation and wake flows normal to the flat solid surface at z = 0 are determined by the following set of regular and singular boundary data:

$$\left. \begin{array}{l} - \infty < r < + \infty \\ z = 0 \end{array} \right\} \quad u = 0, \quad w = 0 \tag{4}$$

$$\left. \begin{array}{l} - \infty \leq r \leq + \infty \\ z \to \infty \end{array} \right\} \quad u \to 0, \quad w \to w_\infty \tag{5}$$

$$\left. \begin{array}{l} r \to \pm \infty \\ z > 0 \end{array} \right\} \quad u \to 0, \quad w \to w_\infty \tag{6}$$

The constant w_∞ is at one's disposal. The motions may be called "stagnation" or "wake" flows according as w_∞ is negative or positive. It may be noted that no boundary data are prescribed at the two singular points ($r = \pm\infty$, $z = 0$) (see Fig. 1).

On the basis of the extended boundary layer theory, which was introduced in [3], the problem under consideration has been reduced to an ordinary boundary value problem in [4]. Its significance for the design of piston machines follows directly from the characterizing boundary data (4), (5), and (6) and Figure 1.

The first order reduction of the Navier-Stokes equations, which is valid for small values of r, was achieved with the aid of the limiting line of the boundary layer along the surface at $z = 0$. In accordance with the extended boundary layer theory (see [3]) this limiting line $z = \delta(r)$ was defined as the solution of the ϵ-equation

$$w(r, z) = w_\infty(1 - \epsilon) \quad . \tag{7}$$

Because of the analyticity and symmetry of the motions $\delta(r)$ must yield an expansion of the form

$$z = \delta(r) = a - br^2 \ldots \tag{8}$$

3

around $r = 0$. Furthermore, it must decrease monotonically to zero as r tends to infinity, i. e., the limiting line of the boundary layer connects the two singular points at $(r = \pm\infty, z = 0)$. While the product

$$ab = \sigma^2 \tag{9}$$

depends on the accuracy parameter ϵ, the ratio

$$\frac{a}{b} = \left(\frac{D}{2}\right)^2 \tag{10}$$

remains as an additional parameter at one's disposal. The value D was roughly identified as the diameter of a flat plate which represents the solid surface of an approximate finite flow model (see Fig. 1). The first order approximation around $r = 0$ was obtained by separation of variables after applying the following similarity transformation:

$$r = r, \qquad \zeta = \frac{z}{\delta(r)} \quad , \qquad R = \frac{w_\infty}{\nu} \sqrt{\frac{a}{b}} \tag{11}$$

$$u = w_\infty \sqrt{\frac{b}{a}} \, rU(\zeta), \quad w = w_\infty W(\zeta), \qquad \frac{p}{\rho} = -\frac{w_\infty^2}{2} P(\zeta) \tag{12}$$

$$U(\zeta) = -\dot{G}(\zeta), \quad W(\zeta) = 2^n \sigma G(\zeta), \quad P(\zeta) = 4^n \sigma^2 H(\zeta) \quad . \tag{13}$$

The constant parameter $|R|$ was found to be the Reynolds number of the flow, which determines the motion uniquely in the (r, ζ) plane.

4

With the transformation (11), (12),and (13) one arrives easily at the following ordinary differential equation for the dimensionless stream function $G(\zeta)$ of the flow (see [4]):

$$\dddot{G} + \sigma^2[(2 + n)4\zeta - (n + 1)RG]\ddot{G} + 2(n + 1)^2\sigma^4\zeta[2\zeta - RG]\dot{G} + \sigma^2R\dot{G}^2 = 0 \quad (14)$$

This differential equation remained to be integrated under the boundary conditions

$$\zeta = 0: \quad G = 0, \quad \dot{G} = 0, \tag{15}$$

$$\zeta = \infty: \quad G = \frac{1}{\sigma(n + 1)} = G_\infty \quad . \tag{16}$$

The pressure function $H(\zeta)$ was then found to be

$$H = 2^{n-1}G^2 - \frac{\dot{G}}{\sigma^2R} + \frac{2(n + 1)}{R} \int\limits_{\zeta}^{\infty} t\dot{G}(t)dt \quad . \tag{17}$$

For a numerical integration of the nonlinear differential equation (14) it is convenient to introduce the following new scales for all variables concerned:

$$\eta = \sigma\zeta , \quad g = \sigma RG , \quad h = \sigma^2R^2H . \tag{18}$$

This leads to the new equation

$$\dddot{g} + [(2 + n)4\eta - (n + 1)g]\ddot{g} + 2(n + 1)^2\eta[2\eta - g]\dot{g} + \dot{g}^2 = 0 , \tag{19}$$

5

which must be integrated under the boundary conditions

$$\eta = 0: \quad g = 0, \quad \dot{g} = 0 \tag{20}$$

$$\eta = \infty: \quad g = g_\infty = \frac{R}{n+1} \quad . \tag{21}$$

The pressure function $h(\zeta)$ is determined by

$$h = 2^{n-1}g^2 - \dot{g} + 2(n+1) \int_\eta^\infty t\dot{g}(t)dt \quad . \tag{22}$$

The advantage of the transformation (18) is evident, as the differential equation (19) may be integrated from a complete set of initial data at $\eta = 0$. The corresponding Reynolds number of the flow is then determined by the boundary condition (21), provided the limiting value g_∞ exists. The remaining initial value problem has been solved by the Runge-Kutta method for a variety of Reynolds numbers. The numerical results will be discussed in the following section.

Since the approximations applied are valid as long as the flow remains laminar and attached to the surface at $z = 0$ at least in the vicinity of the axis of symmetry $r = 0$, it is possible to deal with slow and fast laminar attached motions with stagnation ($w_\infty < 0$) and wake ($w_\infty > 0$) character. This indicates the possibility of detecting those critical Reynolds numbers for which the corresponding laminar flows separate from the surface.

According to physical arguments points of separation may occur in stagnation type flows, but only at some distance from the stagnation point. Thus the extended boundary layer theory can be expected to yield proper results for any finite Reynolds number in the case of stagnation flows. However, points of separation, which may occur farther downstream in stagnation flows, should manifest themselves as points of instability through inflection points in the velocity components parallel to the surface (see, for instance, [1, 2]). In wake type flows the motions are always separated at the wake center provided separation occurs at all. Hence, separation of wake flows should lead to nonexistence of proper solutions to the remaining ordinary boundary value problems, because such flows violate any boundary layer assumption.

The following numerical results will verify the foregoing heuristic observations and, thus, demonstrate probably the most significant justification of the extended boundary layer theory. Indeed, the new boundary layer approximation resolves an old paradox of the classical boundary layer theory. Prandtl's boundary layer assumptions are believed to be best for flows with large Reynolds numbers, that is, for those flows for which in most cases no laminar everywhere attached boundary layer exists. The existence of finite or infinite critical Reynolds numbers contradicts a modern attempt to justify Prandtl's boundary layer approximation

7

which is considered as the leading term of an assumed expansion with respect to the reciprocal Reynolds number (see, e. g., [1]).

3. Properties of Stagnation Flows

The ordinary boundary value problem, which is defined by the equations (19) through (22), has been integrated as an initial value problem by the Runge-Kutta method. Numerical results for axisymmetric (n = 1) and plane (n = 0) stagnation flows (w_∞ < 0) are presented in the tables 1 through 6 for a selected variety of Reynolds numbers. Characteristic examples have been selected and plotted in the figures 2 through 7. These figures display the dimensionless velocity components and the pressure U, W, and P as functions of the dimensionless variable η.

It may be emphasized that the numerical calculations of all stagnation flows computed indicated no symptoms of divergence in the Runge-Kutta method for any Reynolds number. Examples with very large Reynolds numbers have been omitted only because of the very long computing time which such solutions require. Consequently, axisymmetric and plane stagnation flows normal to a flat surface remain laminar and attached at least in the vicinity of their stagnation points at the surface no matter how large the Reynolds number may be chosen. The boundary layer thickness at the stagnation point, which is measured by σ in the (r, η)-plane (see Fig. 2 through 7 and 14), is a decreasing function of the Reynolds number R as long as the flow remains attached to the entire surface.

8

A basic difference between axisymmetric and plane stagnation flows can be observed by comparing the corresponding radial velocities plotted in Figures 2 and 3. The radial velocities of axisymmetric stagnation flows remain free of inflection points within the boundary layer even for very large Reynolds numbers. Hence axisymmetric stagnation flows normal to a flat surface are stable for all finite Reynolds numbers.

In contrast to axisymmetric motions plane stagnation flows normal to a flat surface become unstable as the Reynolds number increases beyond a "critical" value R_c, which has been found to be (see Fig. 5)

$$R_c \approx 54 \ . \tag{23}$$

Hence, in plane stagnation flows separation is to be expected somewhere downstream of the stagnation point, if the Reynolds number passes the critical value (23). Indeed, when the Reynolds number of a plane stagnation flow approaches the critical value (23) one double inflection point occurs in the radial velocity in the lower portion of the boundary layer. As the Reynolds number increases the double inflection point splits into two single inflection points such that the lower point descends to the surface.

The occurrence of two inflection points in the radial velocity of plane stagnation flows contradicts the common description of the phenomenon of flow separation which is based on the classical

9

boundary layer theory (see, e. g., [1, 2]). This reveals a
significant deficiency of Prandtl's boundary layer theory which
destroys intrinsic properties of flows along surfaces. In fact
any flow, which satisfies the Navier-Stokes equations (1)
through (3) and the nonslip condition (4), can be divided into
three different strips:

(I) A "slow motion layer" exists directly at the surface $z = 0$
where any regular flow is essentially governed by the so-called
Stokes equations, which neglect all inertial forces as terms of
second and higher order in z.

(II) A "fast motion layer" exists at large distances from the sur-
face, where the flow is essentially determined by the Euler
equations, which ignore all friction forces (boundary layer
assumption).

(III) A "transition layer" joins the slow motion layer with the
fast motion region, where the flow is governed by the complete
Navier-Stokes equations.

As generally acknowledged the classical boundary layer theory
is not applicable to slow motions and, hence, presents itself as
inadequate to describe the phenomenon of flow separation which
originates in the lower part of the transition layer. If the fast
motion at some distance from the surface tends to surpass the
slow motion at the surface, an instability develops in the

10

transition layer which spreads gradually across the slow motion layer and causes the flow separation when the surface is reached.

4. Properties of Wake Flows

Axisymmetric and plane wake ($w_\infty > 0$) flows normal to a flat surface have been computed and tabulated for various Reynolds numbers (see Tables 7 through 12). Characteristic examples have been selected and plotted in the figures 8 through 13.

As anticipated in section 2 solutions were only computable for relatively small Reynolds numbers. If the Reynolds number approaches a "critical" value, which has been found to be

$$R_a \approx 6.6 \text{ for axisymmetric flows} \tag{24}$$

and

$$\hat{R}_p \approx 4.8 \text{ for plane flow,} \tag{25}$$

one double inflection point occurs in the radial velocity (see Fig. 8 and 11) in the upper portion of the boundary layer. If the Reynolds number increases beyond its critical value the double inflection point splits into two single inflection points where the upper point ascends very rapidly to infinity and a proper solution ceases to exist.

In contrast to plane stagnation flows separation originates in wake flows in the upper portion of the boundary layer. An instability occurs in the transition layer and spreads very rapidly across the fast motion region. At the same time the

11

boundary layer thickness grows beyond any limits (see Fig. 8

through 13 and 15) and the existence of a laminar boundary layer

is no longer possible.

REFERENCES

[1] Meksyn, D., New Methods in Laminar Boundary-Layer Theory, Pergamon Press, 1961.

[2] Schlichting, H., Boundary Layer Theory, Fourth Edition, 1960.

[3] Schwiderski, E. W., and Lugt, H., Boundary Layer Along a Flat Surface Normal to a Vortex Flow, U. S. Naval Weapons Laboratory Report No. 1835, 1962.

[4] Schwiderski, E. W., and Lugt, H., Rotating Flows of Kármán-Bödewadt and Stagnation Flows, U. S. Naval Weapons Laboratory Report No. 1836, 1962.

APPENDIX A

TABLE 1

RADIAL VELOCITY U OF AXISYMMETRIC STAGNATION FLOWS

R	.6982	6.028	46.84	412.4	3974
$R\dfrac{dU}{d\eta}$	-1	-10	-100	-10^3	-10^4
σ	2.15	1.85	1.50	1.41	1.40
η					
0	.0000	.0000	.0000	.0000	.0000
.1	.1404	.1626	.2093	.2376	.2461
.2	.2648	.3066	.3943	.4450	.4562
.3	.3611	.4179	.5344	.5917	.6007
.4	.4239	.4895	.6157	.6622	.6673
.5	.4539	.5211	.6341	.6598	.6608
.6	.4562	.5174	.5971	.6009	.5986
.7	.4377	.4862	.5222	.5075	.5030
.8	.4053	.4361	.4280	.4013	.3958
.9	.3648	.3757	.3315	.2995	.2939
1.0	.3204	.3122	.2440	.2118	.2068
1.1	.2754	.2512	.1714	.1427	.1385
1.2	.2322	.1961	.1155	.0917	.0885
1.3	.1922	.1491	.0748	.0565	.0541
1.4	.1561	.1106	.0467	.0333	.0317
1.5	.1247	.0802	.0281	.0189	.0178
1.6	.0980	.0569	.0164	.0103	.0096
1.7	.0756	.0395	.0092	.0054	.0050
1.8	.0575	.0270	.0051	.0027	.0025
1.9	.0430	.0180	.0027	.0013	.0012
2.0	.0316	.0119	.0014	.0006	.0005
2.2	.0163	.0049	.0003		
2.4	.0079	.0019	.0007		
2.6	.0036	.0007			
2.8	.0015	.0002			
3.0	.0006	.0001			
3.4	.0001				

TABLE 2

AXIAL VELOCITY W OF AXISYMMETRIC STAGNATION FLOWS

$|R|$	.6982	6.028	46.84	412.4	3974
$R\frac{dU}{d\eta}$	-1	-10	-100	-10^3	-10^4
η \ σ	2.15	1.85	1.50	1.41	1.40
0	.0000	.0000	.0000	.0000	.0000
.1	.0142	.0164	.0211	.0240	.0249
.2	.0551	.0638	.0821	.0931	.0960
.3	.1182	.1369	.1758	.1979	.2030
.4	.1973	.2283	.2919	.3249	.3311
.5	.2856	.3300	.4179	.4579	.4650
.6	.3770	.4343	.5418	.5849	.5918
.7	.4660	.5352	.6541	.6959	.7021
.8	.5511	.6277	.7494	.7871	.7921
.9	.6282	.7090	.8254	.8569	.8611
1.0	.6969	.7777	.8826	.9079	.9109
1.1	.7565	.8338	.9240	.9428	.9451
1.2	.8072	.8786	.9522	.9661	.9673
1.3	.8496	.9131	.9710	.9806	.9814
1.4	.8843	.9386	.9829	.9893	.9899
1.5	.9123	.9579	.9902	.9942	.9946
1.6	.9344	.9711	.9949	.9971	.9974
1.7	.9519	.9808	.9974	.9988	.9990
1.8	.9651	.9874	.9987	.9995	.9996
1.9	.9751	.9920	.9996	1.0000	1.0000
2.0	.9822	.9947	.9996		
2.2	.9917	.9980	1.0000		
2.4	.9963	.9993			
2.6	.9986	.9997			
2.8	.9994	1.0000			
3.0	1.0000				

TABLE 3

PRESSURE DISTRIBUTION P OF AXISYMMETRIC STAGNATION FLOWS

$\lvert R \rvert$	.6982	6.028	46.84	412.4	3974
$R\dfrac{dU}{d\eta}$	-1	-10	-100	-10^3	-10^4
σ	2.5	1.85	1.50	1.41	1.40
η					
0	-9.388	-.9559	-.1033	-.0111	-.0011
.1	-8.567	-.8463	-.0848	-.0082	-.0003
.2	-7.774	-.7371	-.0611	+.0002	+.0086
.3	-7.022	-.6240	-.0209	.0346	.0408
.4	-6.314	-.5004	+.0473	.1023	.1093
.5	-5.639	-.3619	.1480	.2077	.2161
.6	-4.984	-.2083	.2753	.3407	.3500
.7	-4.343	-.0444	.4158	.4837	.4931
.8	-3.712	+.1219	.5534	.6189	.6276
.9	-3.099	.2819	.6757	.7338	.7414
1.0	-2.513	.4284	.7754	.8237	.8295
1.1	-1.964	.5573	.8511	.8885	.8931
1.2	-1.462	.6652	.9052	.9438	.9359
1.3	-1.008	.7522	.9419	.9612	.9633
1.4	- .6198	.8216	.9655	.9786	.9800
1.5	- .2810	.8733	.9803	.9887	.9894
1.6	.0000	.9119	.9891	.9944	.9947
1.7	+ .2397	.9405	.9942	.9974	.9990
1.8	.4215	.9604	.9969	.9988	.9997
1.9	.5702	.9736	.9996	.9998	1.0000
2.0	.6860	.9835	.9996	1.0000	
2.2	.8430	.9934	1.0000		
2.4	.9256	.9978			
2.6	.9669	1.0000			
2.8	.9917				
3.0	1.0000				

TABLE 4

HORIZONTAL VELOCITY U OF PLANE STAGNATION FLOWS

$/R/$	.7127	6.697	53.59	100.2	11700
$R\frac{dU}{d\eta}$	-1	-10	-64	-100	-1000
σ / η	3.51	2.85	2.27	2.22	2.27
0	.0000	.0000	.0000	.0000	.0000
.1	.1385	.1474	.1182	.0989	.0088
.2	.2663	.2843	.2314	.1955	.0213
.3	.3752	.4030	.3402	.2941	.0454
.4	.4602	.4999	.4480	.4006	.0909
.5	.5201	.5740	.5551	.5159	.1683
.6	.5566	.6263	.6568	.6333	.2862
.7	.5736	.6581	.7442	.7040	.4441
.8	.5751	.6715	.8067	.8233	.6274
.9	.5653	.6684	.8365	.8695	.8079
1.0	.5475	.6504	.8300	.8728	.9513
1.1	.5238	.6200	.7886	.8343	1.0300
1.2	.4964	.5798	.7190	.7613	1.0320
1.3	.4664	.5323	.6307	.6654	.9658
1.4	.4348	.4805	.5339	.5589	.8491
1.5	.4024	.4269	.4374	.4529	.7071
1.6	.3699	.3736	.3476	.3529	.5615
1.7	.3376	.3224	.2689	.2701	.4276
1.8	.3062	.2747	.2030	.2001	.3140
1.9	.2759	.2313	.1498	.1446	.2232
2.0	.2469	.1926	.1082	.1022	.1542
2.2	.1943	.1295	.0534	.0479	.0681
2.4	.1493	.0839	.0246	.0208	.0274
2.6	.1120	.0527	.0107	.0084	.0101
2.8	.0821	.0321	.0044	.0032	.0034
3.0	.0588	.0190	.0017	.0011	.0011
3.4	.0283	.0062	.0002	.0001	
3.8	.0124	.0018			
4.2	.0050	.0050			
4.6	.0019	.0001			
5.0	.0006				

TABLE 5

VERTICAL VELOCITY W OF PLANE STAGNATION FLOWS

/R/	.7127	6.697	53.59	100.2	11700
$R \frac{dU}{d\eta}$	-1	-10	-64	-100	-1000
σ η	3.51	2.85	2.27	2.22	2.27
0	.0000	.0000	.0000	.0000	.0000
.1	.0070	.0074	.0059	.0050	.0004
.2	.0273	.0291	.0235	.0197	.0019
.3	.0596	.0637	.0521	.0441	.0051
.4	.1016	.1090	.0915	.0788	.0117
.5	.1508	.1629	.1416	.1246	.0243
.6	.2049	.2231	.2023	.1820	.0467
.7	.2615	.2874	.2724	.2509	.0829
.8	.3191	.3540	.3503	.3293	.1364
.9	.3762	.4212	.4327	.4143	.2083
1.0	.4319	.4872	.5163	.5018	.2968
1.1	.4855	.5508	.5975	.5874	.3964
1.2	.5364	.6109	.6733	.6675	.5002
1.3	.5847	.6666	.7408	.7389	.6006
1.4	.6297	.7172	.7990	.8002	.6916
1.5	.6715	.7626	.8475	.8507	.7696
1.6	.7101	.8026	.8867	.8910	.8330
1.7	.7455	.8374	.9175	.9222	.8821
1.8	.7777	.8673	.9410	.9455	.9188
1.9	.8068	.8925	.9586	.9627	.9462
2.0	.8329	.9137	.9713	.9749	.9650
2.2	.8769	.9455	.9869	.9893	.9855
2.4	.9112	.9667	.9944	.9959	.9949
2.6	.9371	.9801	.9978	.9990	.9983
2.8	.9564	.9884	.9993	1.0000	.9991
3.0	.9704	.9934	.9998		1.0000
3.4	.9872	.9981	1.0000		
3.8	.9949	.9994			
4.2	.9983	.9999			
4.6	.9996	1.0000			
5.0	1.0000				

TABLE 6

PRESSURE DISTRIBUTION P OF PLANE STAGNATION FLOWS

/R/	.7127	6.697	53.59	100.2	11700
$R \frac{dU}{d\eta}$	-1	-10	-64	-100	-1000
σ	3.51	2.85	2.27	2.22	2.27
η					
0	-7.075	-.6589	-.0756	-.0409	-.0004
.1	-6.685	-.6146	-.0711	-.0389	-.0004
.2	-6.309	-.5709	-.0662	-.0365	-.0004
.3	-5.957	-.5270	-.0594	-.0328	-.0004
.4	-5.629	-.4807	-.0487	-.0259	-.0003
.5	-5.326	-.4295	-.0313	-.0135	+.0002
.6	-5.038	-.3708	-.0042	+.0078	.0018
.7	-4.758	-.3035	+.0358	.0415	.0065
.8	-4.480	-.2269	.0909	.0910	.0183
.9	-4.196	-.1418	.1618	.1580	.0432
1.0	-3.906	-.0495	.2469	.2415	.0879
1.1	-3.608	+.0473	.3421	.3376	.1569
1.2	-3.305	.1462	.4420	.4402	.2500
1.3	-3.000	.2448	.5406	.5424	.3606
1.4	-2.694	.3402	.6324	.6378	.4784
1.5	-2.388	.4302	.7139	.7220	.5922
1.6	-2.094	.5140	.7828	.7927	.6939
1.7	-1.808	.5903	.8392	.8494	.7785
1.8	-1.529	.6580	.8837	.8933	.8450
1.9	-1.271	.7173	.9172	.9261	.8947
2.0	-1.024	.7686	.9422	.9500	.9305
2.2	- .5804	.8489	.9735	.9783	.9718
2.4	- .2039	.9046	.9882	.9914	.9896
2.6	+ .1020	.9412	.9951	.9970	.9966
2.8	+ .3451	.9648	.9979	.9992	.9991
3.0	.5333	.9795	.9993	1.0000	1.0000
3.4	.7804	.9933	1.0000		
3.8	.9059	.9982			
4.2	.9647	.9996			
4.6	.9882	1.0000			
5.0	1.0000				

TABLE 7

RADIAL VELOCITY U OF AXISYMMETRIC WAKE FLOWS

R	.0720	.7412	1.539	3.414	6.554	8.692
$R \frac{dU}{d\eta}$	.1	1	2	4	6.2	7
σ η	2.23	2.29	2.38	2.62	3.14	3.55
0	.0000	.0000	.0000	.0000	.0000	.0000
.1	.1362	.1323	.1274	.1149	.0927	.0790
.2	.2568	.2495	.2402	.2166	.1749	.1489
.3	.3503	.3403	.3277	.2955	.2386	.2032
.4	.4112	.3996	.3850	.3474	.2807	.2391
.5	.4407	.4285	.4131	.3735	.3023	.2575
.6	.4436	.4320	.4171	.3781	.3073	.2622
.7	.4269	.4168	.4035	.3682	.3012	.2578
.8	.3972	.3894	.3787	.3489	.2890	.2485
.9	.3599	.3548	.3475	.3248	.2740	.2373
1.0	.3189	.3169	.3133	.2991	.2586	.2262
1.1	.2774	.2782	.2782	.2723	.2435	.2158
1.2	.2368	.2403	.2437	.2460	.2289	.2063
1.3	.1989	.2044	.2105	.2203	.2148	.1975
1.4	.1643	.1713	.1795	.1954	.2013	.1893
1.5	.1335	.1414	.1510	.1716	.1877	.1811
1.6	.1067	.1149	.1252	.1491	.1742	.1731
1.7	.0840	.0920	.1023	.1281	.1607	.1650
1.8	.0651	.0725	.0824	.1086	.1472	.1566
1.9	.0496	.0563	.0654	.0910	.1337	.1481
2.0	.0372	.0430	.0511	.0752	.1204	.1392
2.2	.0200	.0240	.0299	.0492	.0948	.1206
2.4	.0101	.0126	.0164	.0304	.0713	.1013
2.6	.0048	.0062	.0085	.0177	.0510	.0819
2.8	.0021	.0029	.0041	.0096	.0345	.0635
3.0	.0009	.0012	.0019	.0050	.0220	.0468
3.4	.0001	.0002	.0003	.0011	.0074	.0215
3.8				.0002	.0019	.0077
4.2					.0004	.0021
4.6					.0001	.0005
5.0						.0001

TABLE 8

AXIAL VELOCITY W OF AXISYMMETRIC WAKE FLOWS

$\|R\|$	.0720	.7412	1.539	3.414	6.554	8.692
$/R\,\dfrac{dU}{d\eta}$	.1	1	2	4	6.2	7
σ	2.23	2.29	2.38	2.62	3.14	3.55
η						
0	.0000	.0000	.0000	.0000	.0000	.0000
.1	.0138	.0134	.0129	.0116	.0094	.0080
.2	.0534	.0519	.0500	.0451	.0364	.0310
.3	.1146	.1114	.1072	.0967	.0781	.0665
.4	.1913	.1859	.1790	.1615	.1304	.1110
.5	.2770	.2692	.2593	.2339	.1890	.1609
.6	.3658	.3556	.3426	.3094	.2502	.2131
.7	.4531	.4406	.4250	.3842	.3113	.2653
.8	.5358	.5216	.5033	.4561	.3702	.3159
.9	.6117	.5961	.5761	.5235	.4266	.3645
1.0	.6794	.6632	.6421	.5858	.4800	.4107
1.1	.7392	.7226	.7013	.6432	.5301	.4549
1.2	.7906	.7744	.7534	.6948	.5774	.4972
1.3	.8339	.8189	.7989	.7417	.6216	.5375
1.4	.8703	.8564	.8377	.7832	.6634	.5762
1.5	.9000	.8877	.8707	.8196	.7022	.6132
1.6	.9239	.9131	.8984	.8518	.7385	.6486
1.7	.9428	.9339	.9210	.8793	.7717	.6825
1.8	.9578	.9504	.9395	.9033	.8026	.7147
1.9	.9692	.9630	.9541	.9233	.8306	.7451
2.0	.9778	.9730	.9658	.9397	.8560	.7738
2.2	.9889	.9860	.9817	.9643	.8990	.8258
2.4	.9947	.9933	.9908	.9801	.9323	.8702
2.6	.9975	.9968	.9956	.9895	.9567	.9068
2.8	.9989	.9987	.9981	.9947	.9735	.9358
3.0	.9994	.9995	.9991	.9977	.9847	.9579
3.4	.9997	.9997	.9999	.9994	.9957	.9844
3.8	1.0000	1.0000	1.0000	1.0000	.9991	.9954
4.2					.9997	.9988
4.6					1.0000	.9998
5.0						1.0000

TABLE 9

PRESSURE DISTRIBUTION P OF AXISYMMETRIC WAKE FLOWS

R	.0720	.7412	1.539	3.414	6.554	8.692
$R \dfrac{dU}{d\eta}$	.1	1	2	4	6.2	7
σ	2.23	2.29	2.38	2.62	3.14	3.55
η						
0	92.46	9.196	4.594	2.271	1.432	1.246
.1	84.82	8.4759	4.259	2.135	1.375	1.210
.2	77.46	7.7848	3.938	2.006	1.321	1.175
.3	70.58	7.146	3.645	1.890	1.274	1.145
.4	64.24	6.567	3.386	1.793	1.236	1.122
.5	58.37	6.047	3.160	1.714	1.210	1.107
.6	52.85	5.571	2.962	1.652	1.192	1.098
.7	47.57	5.126	2.782	1.602	1.182	1.093
.8	42.44	4.701	2.616	1.559	1.176	1.092
.9	37.46	4.290	2.454	1.519	1.171	1.092
1.0	32.68	3.892	2.297	1.480	1.167	1.093
1.1	28.15	3.512	2.145	1.441	1.163	1.093
1.2	23.92	3.153	2.000	1.401	1.158	1.093
1.3	20.08	2.820	1.862	1.362	1.152	1.092
1.4	16.65	2.517	1.734	1.323	1.145	1.091
1.5	13.62	2.246	1.616	1.285	1.138	1.090
1.6	11.08	2.009	1.509	1.249	1.130	1.088
1.7	8.846	1.804	1.417	1.214	1.121	1.085
1.8	7.077	1.630	1.334	1.183	1.112	1.082
1.9	5.615	1.486	1.265	1.153	1.103	1.078
2.0	4.462	1.370	1.207	1.127	1.093	1.075
2.2	2.846	1.203	1.121	1.083	1.057	1.066
2.4	1.923	1.109	1.066	1.052	1.041	1.056
2.6	1.462	1.051	1.034	1.030	1.028	1.046
2.8	1.231	1.022	1.017	1.016	1.018	1.036
3.0	1.077	1.007	1.007	1.009	1.006	1.027
3.4	1.000	1.000	1.002	1.002	1.002	1.013
3.8			1.000	1.000	1.000	1.005
4.2						1.001
4.6						1.000
5.0						

TABLE 10

HORIZONTAL VELOCITY U OF PLANE WAKE FLOWS

R	.0728	.7443	1.536	3.378	4.831	6.139
$R\frac{dU}{d\eta}$	.1	1	2	4	5.2	6
σ	3.659	3.785	3.965	4.37	4.62	4.78
η						
0	.0000	.0000	.0000	.0000	.0000	.0000
.1	.1355	.1326	.1285	.1168	.1062	.0964
.2	.2607	.2549	.2469	.2244	.2039	.1850
.3	.3668	.3586	.3471	.3150	.2861	.2595
.4	.4494	.4387	.4241	.3840	.3480	.3154
.5	.5068	.4939	.4766	.4298	.3887	.3517
.6	.5410	.5261	.5066	.4547	.4101	.3703
.7	.5560	.5396	.5182	.4627	.4159	.3747
.8	.5562	.5386	.5161	.4586	.4109	.3694
.9	.5457	.5276	.5047	.4467	.3993	.3584
1.0	.5279	.5101	.4876	.4307	.3846	.3450
1.1	.5056	.4886	.4673	.4133	.3691	.3312
1.2	.4800	.4647	.4452	.3952	.3540	.3181
1.3	.4525	.4395	.4223	.3777	.3397	.3062
1.4	.4238	.4134	.3992	.3606	.3264	.2957
1.5	.3947	.3869	.3760	.3443	.3142	.2862
1.6	.3655	.3606	.3530	.3283	.3026	.2777
1.7	.3365	.3344	.3302	.3126	.2917	.2698
1.8	.3081	.3087	.3077	.2972	.2811	.2623
1.9	.2805	.2836	.2857	.2823	.2708	.2553
2.0	.2539	.2593	.2641	.2674	.2606	.2482
2.2	.2048	.2136	.2230	.2382	.2403	.2349
2.4	.1617	.1725	.1850	.2098	.2202	.2214
2.6	.1247	.1365	.1507	.1824	.2001	.2077
2.8	.0942	.1058	.1205	.1563	.1800	.1935
3.0	.0696	.0803	.0945	.1319	.1600	.1789
3.4	.0356	.0434	.0546	.0892	.1214	.1485
3.8	.0167	.0216	.0291	.0560	.0866	.1177
4.2	.0072	.0098	.0142	.0325	.0576	.0880
4.6	.0028	.0041	.0064	.0173	.0355	.0616
5.0	.0010	.0016	.0026	.0085	.0201	.0401

TABLE 11

VERTICAL VELOCITY W OF PLANE WAKE FLOWS

R	.0728	.7443	1.536	3.378	4.831	6.139
$R\frac{dU}{d\eta}$	.1	1	2	4	5.2	6
σ	3.659	3.785	3.965	4.37	4.62	4.78
η						
0	.0000	.0000	.0000	.0000	.0000	.0000
.1	.0068	.0067	.0065	.0059	.0053	.0049
.2	.0268	.0262	.0254	.0231	.0209	.0190
.3	.0583	.0570	.0552	.0502	.0456	.0414
.4	.0993	.0971	.0940	.0854	.0775	.0703
.5	.1474	.1439	.1393	.1262	.1145	.1038
.6	.2000	.1951	.1886	.1706	.1546	.1400
.7	.2549	.2486	.2400	.2166	.1960	.1774
.8	.3107	.3026	.2917	.2627	.2374	.2147
.9	.3657	.3559	.3428	.3079	.2780	.2510
1.0	.4196	.4079	.3925	.3520	.3171	.2862
1.1	.4712	.4579	.4403	.3940	.3548	.3201
1.2	.5205	.5054	.4859	.4346	.3910	.3525
1.3	.5672	.5507	.5293	.4731	.4256	.3838
1.4	.6110	.5933	.5704	.5101	.4589	.4137
1.5	.6520	.6333	.6091	.5453	.4910	.4429
1.6	.6899	.6707	.6456	.5790	.5218	.4711
1.7	.7250	.7055	.6797	.6110	.5514	.4985
1.8	.7573	.7376	.7116	.6415	.5802	.5250
1.9	.7867	.7673	.7415	.6705	.6077	.5509
2.0	.8133	.7944	.7689	.6980	.6342	.5762
2.2	.8592	.8416	.8177	.7484	.6843	.6244
2.4	.8958	.8802	.8581	.7934	.7305	.6700
2.6	.9242	.9109	.8919	.8324	.7725	.7130
2.8	.9460	.9351	.9186	.8662	.8106	.7531
3.0	.9624	.9536	.9401	.8952	.8445	.7904
3.4	.9827	.9777	.9694	.9390	.9006	.8558
3.8	.9929	.9903	.9857	.9677	.9420	.9091
4.2	.9974	.9964	.9941	.9852	.9708	.9502
4.6	.9993	.9991	.9980	.9950	.9892	.9800
5.0	1.0000	1.0000	1.0000	1.0000	1.0000	1.0000

TABLE 12

PRESSURE DISTRIBUTION P OF PLANE WAKE FLOWS

R	.0728	.7443	1.536	3.378	4.831	6.139
$R\dfrac{dU}{d\eta}$	.1	1	2	4	5.2	6
σ $\diagdown$ η	3.659	3.785	3.965	4.37	4.62	4.73
0	73.19	7.272	3.674	1.876	1.458	1.256
.1	69.37	6.912	3.505	1.806	1.413	1.234
.2	65.70	6.566	3.343	1.739	1.371	1.204
.3	62.28	6.247	3.195	1.679	1.333	1.177
.4	59.17	5.962	3.064	1.628	1.302	1.155
.5	56.36	5.710	2.953	1.588	1.278	1.139
.6	53.80	5.488	2.859	1.557	1.262	1.129
.7	51.40	5.289	2.779	1.535	1.251	1.123
.8	49.08	5.103	2.707	1.518	1.246	1.121
.9	46.79	4.923	2.642	1.505	1.243	1.122
1.0	44.47	4.744	2.577	1.494	1.241	1.123
1.1	42.11	4.562	2.512	1.484	1.240	1.125
1.2	39.70	4.377	2.447	1.473	1.239	1.127
1.3	37.26	4.189	2.379	1.461	1.237	1.128
1.4	34.80	3.998	2.310	1.448	1.235	1.129
1.5	32.35	3.805	2.239	1.434	1.232	1.130
1.6	29.29	3.612	2.168	1.420	1.228	1.130
1.7	27.54	3.424	2.095	1.405	1.224	1.130
1.8	25.23	3.236	2.023	1.389	1.220	1.129
1.9	23.00	3.051	1.953	1.372	1.214	1.128
2.0	20.85	2.873	1.882	1.355	1.209	1.127
2.2	16.96	2.540	1.746	1.320	1.196	1.123
2.4	13.54	2.243	1.620	1.284	1.182	1.118
2.6	10.62	1.978	1.505	1.247	1.166	1.112
2.8	8.231	1.757	1.402	1.212	1.149	1.105
3.0	6.308	1.572	1.314	1.178	1.132	1.096
3.4	3.654	1.304	1.179	1.118	1.098	1.077
3.8	2.192	1.145	1.092	1.070	1.065	1.057
4.2	1.462	1.058	1.041	1.036	1.037	1.035
4.6	1.115	1.018	1.014	1.014	1.015	1.016
5.0	1.000	1.000	1.000	1.000	1.000	1.000

APPENDIX B

$w_{(z = \infty)}$ = finite

$u_{(r=\infty \atop z=0)}$ = ∞
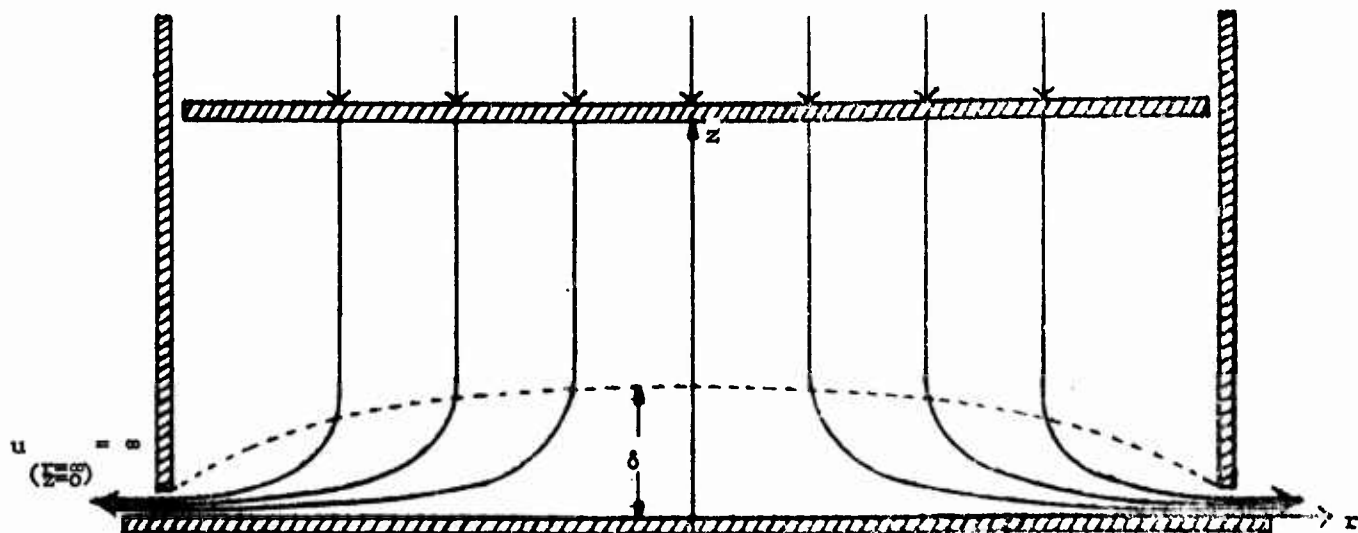
FIGURE 1a: Model of the stagnation flow "normal" to a plate.

$w_{(z = \infty)}$ = ∞

$u_{(r = \infty)}$ = ∞
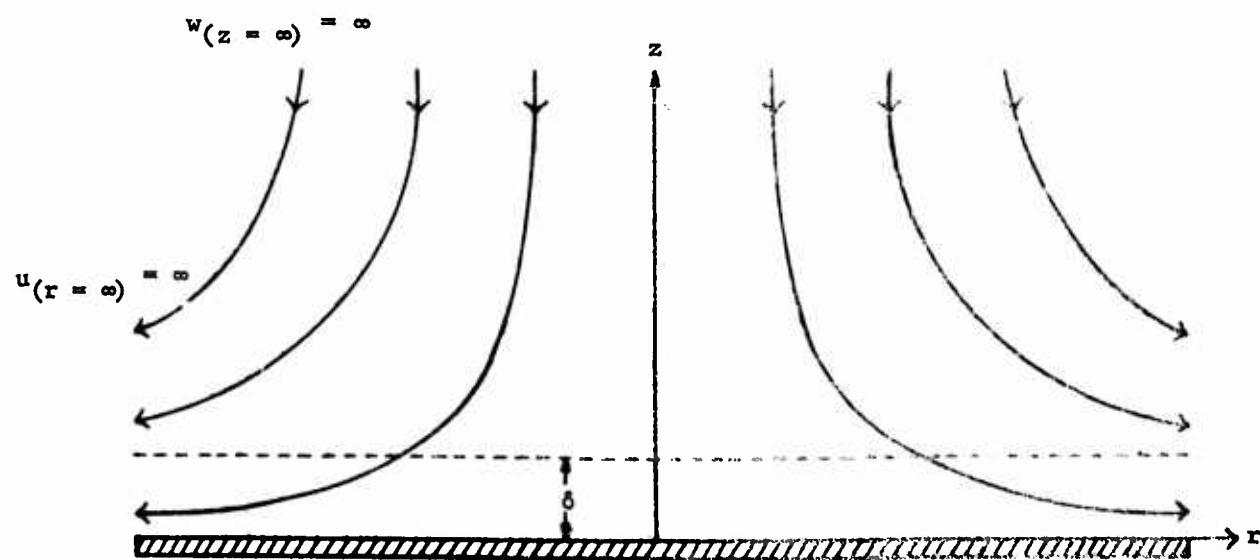
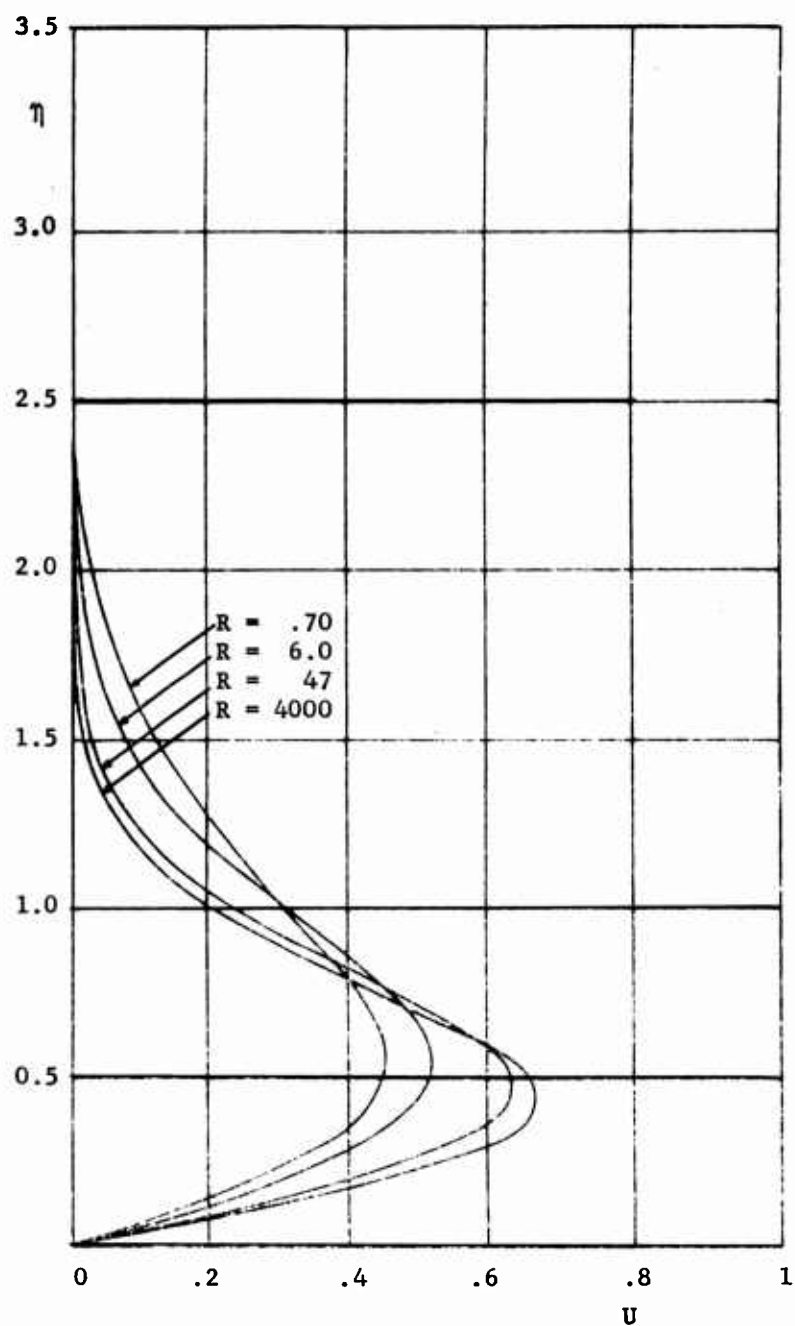FIGURE 1b: Model of the classical stagnation flow "past" a plate.

FIGURE 2: The radial velocity U of axisymmetric stagnation flows vs. the dimensionless variable η for four different Reynolds numbers R.
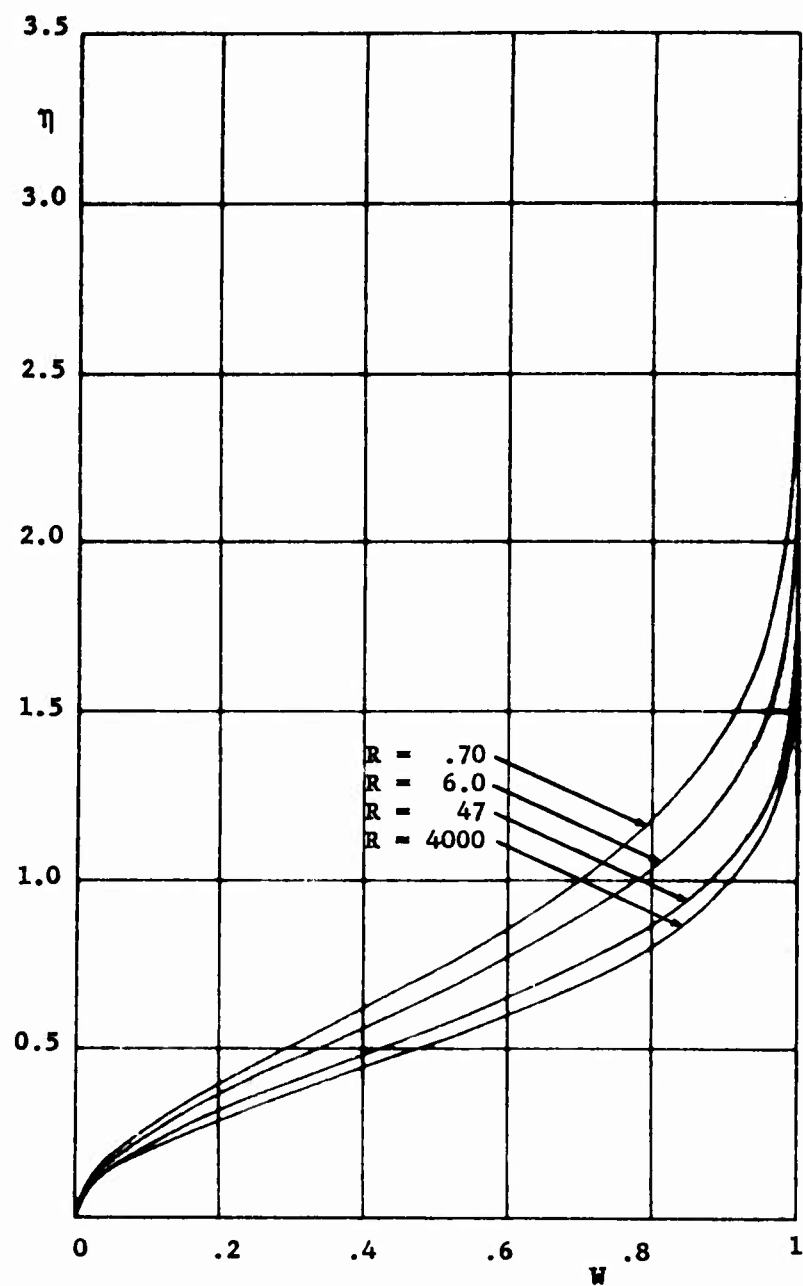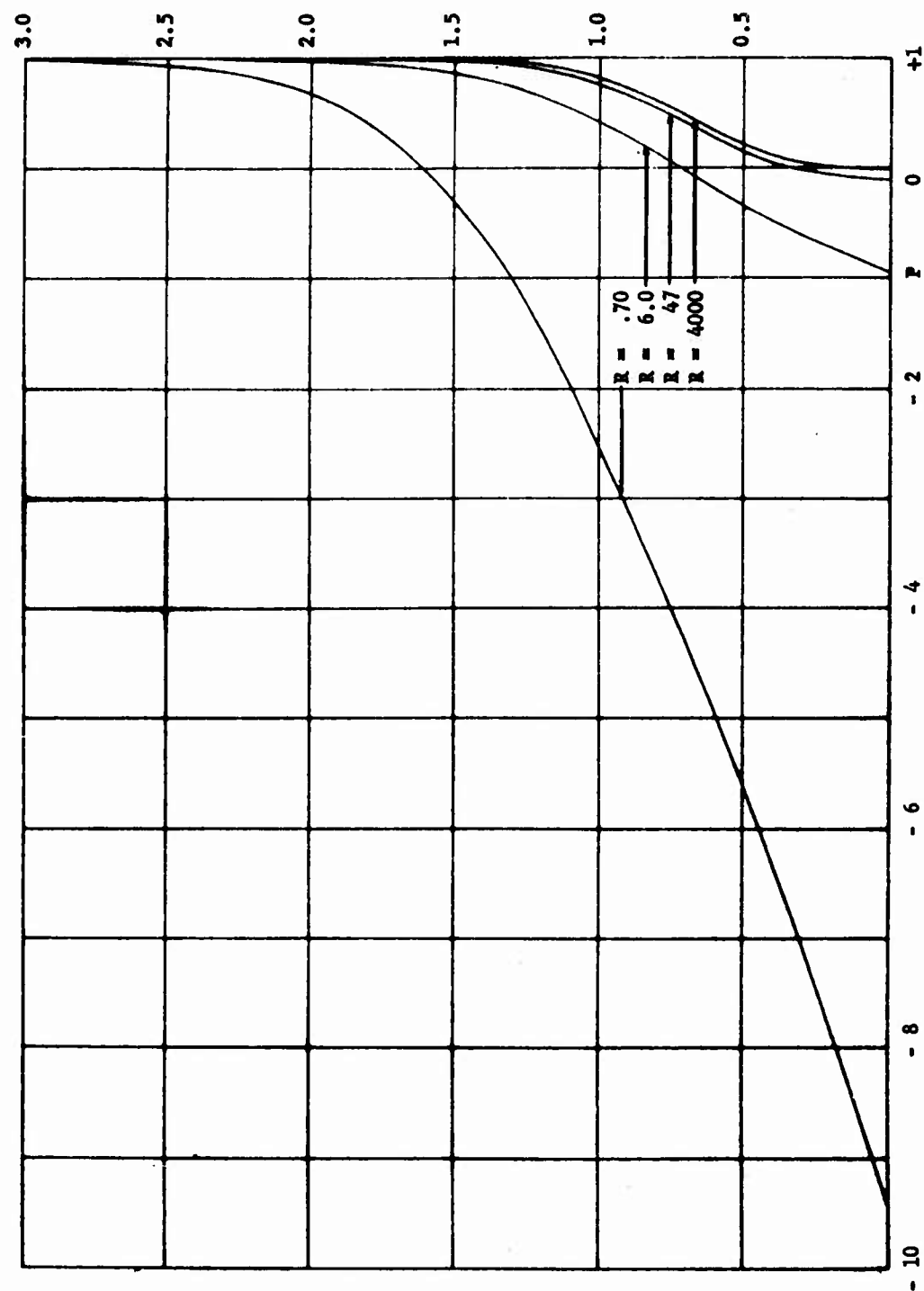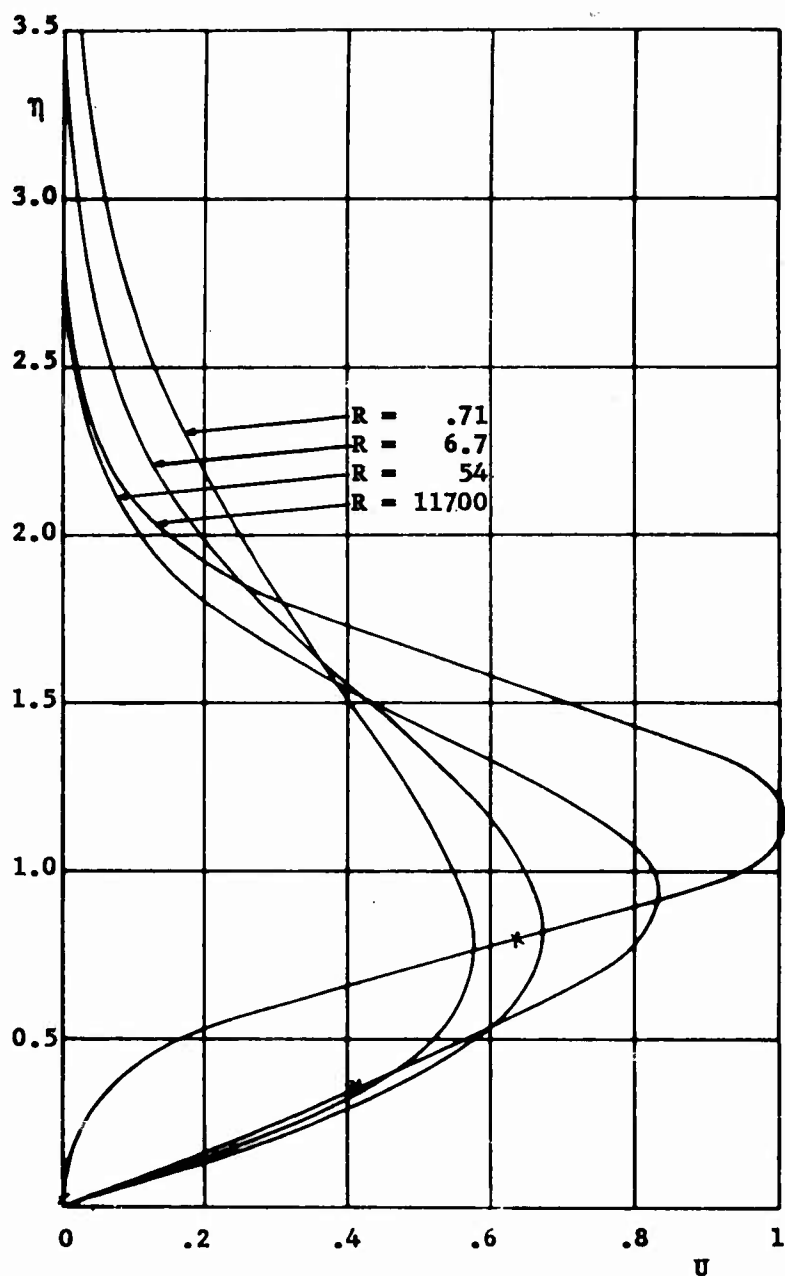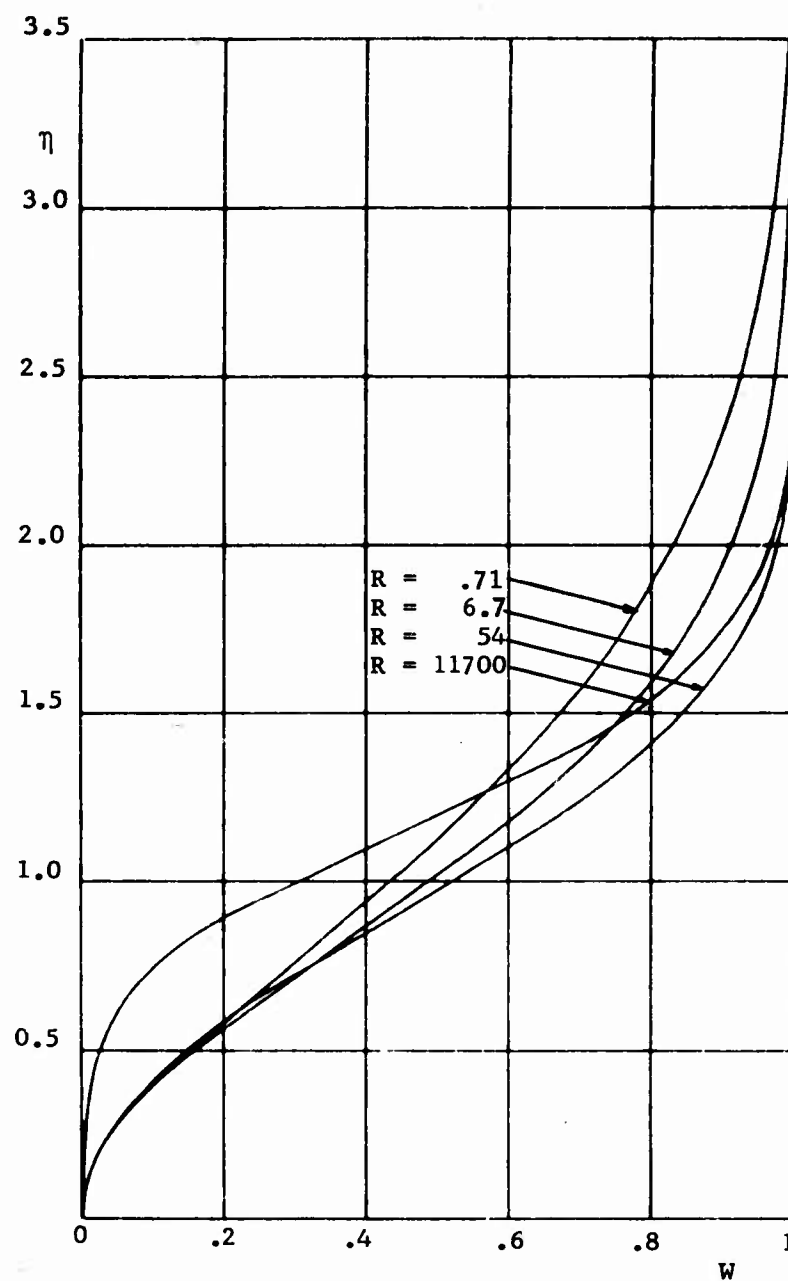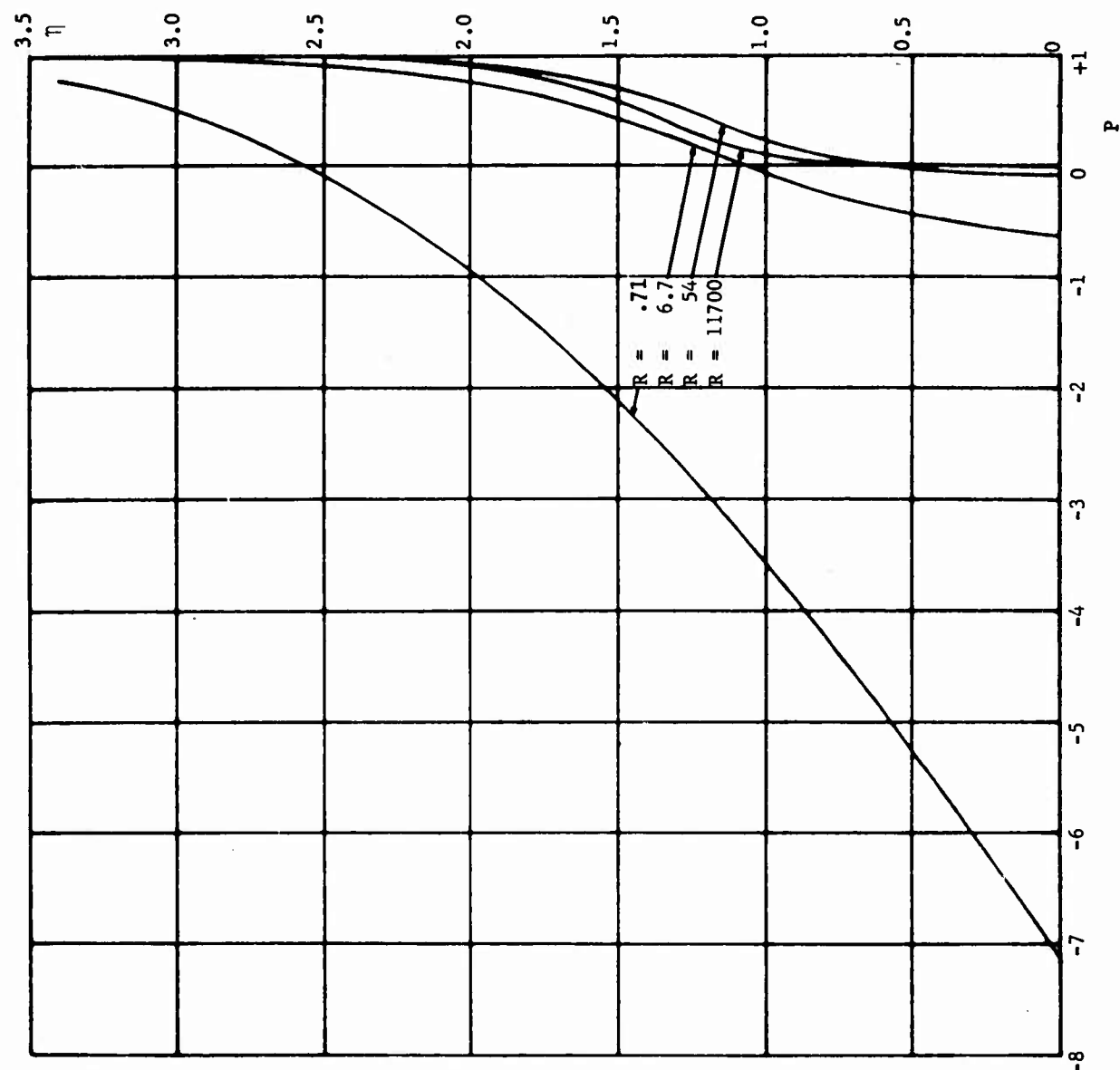
FIGURE 3: The axial velocity W of axisymmetric stagnation flows vs the dimensionless variable η for four different Reynolds numbers R.

FIGURE 4: Pressure distribution P of axisymmetric stagnation flows vs. the dimensionless variable η for four different Reynolds numbers R.
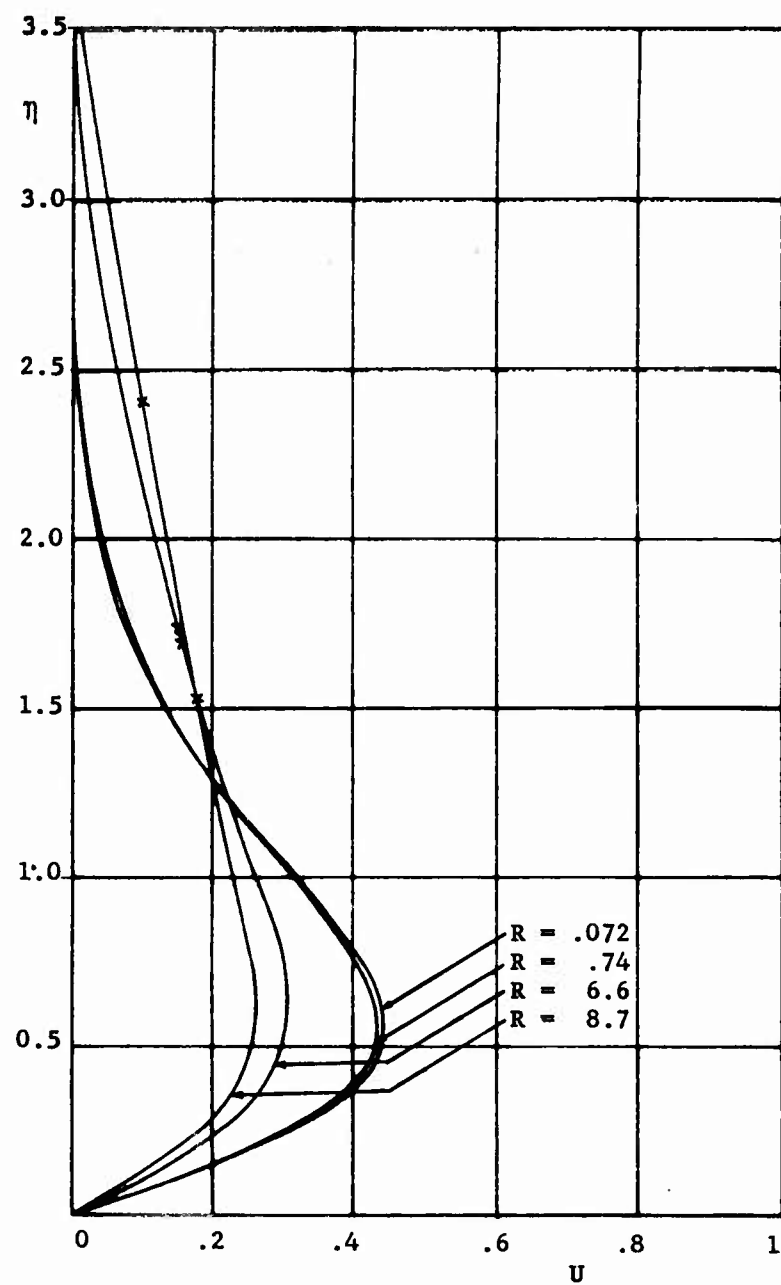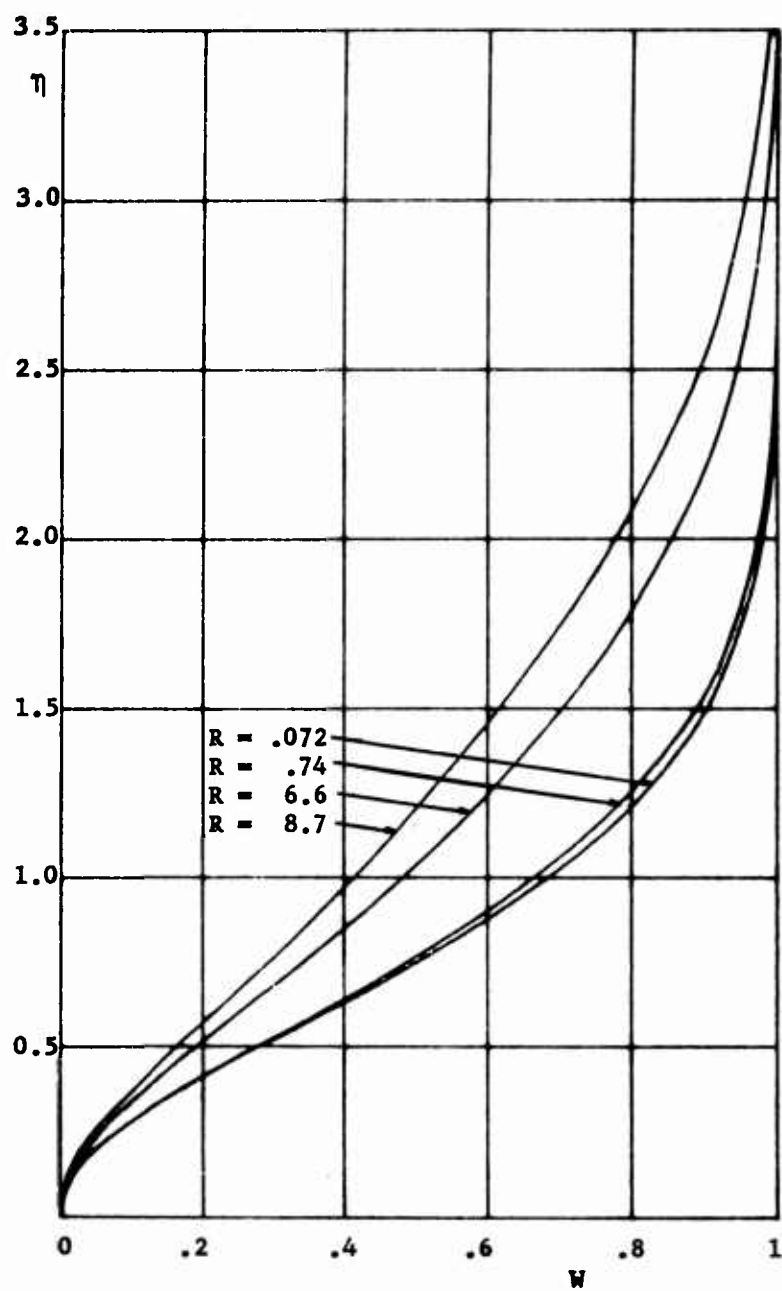
FIGURE 5: The horizontal velocity U of plane stagnation flows vs. the dimensionless variable η for four different Reynolds numbers R. (*Inflection point of instability)

FIGURE 6: The vertical velocity W of plane stagnation flows vs. the dimensionless variable η for four different Reynolds numbers R.

FIGURE 7: Pressure distribution P of plane stagnation flows vs. the dimensionless variable η for four different Reynolds numbers R.

FIGURE 8: The radial velocity U of axisymmetric wake flows vs.
the dimensionless variable η for four different
Reynolds numbers R. (*Inflection point of instability)

FIGURE 9: The axial velocity W of axisymmetric wake flows vs. the dimensionless variable η for four different Reynolds numbers R.
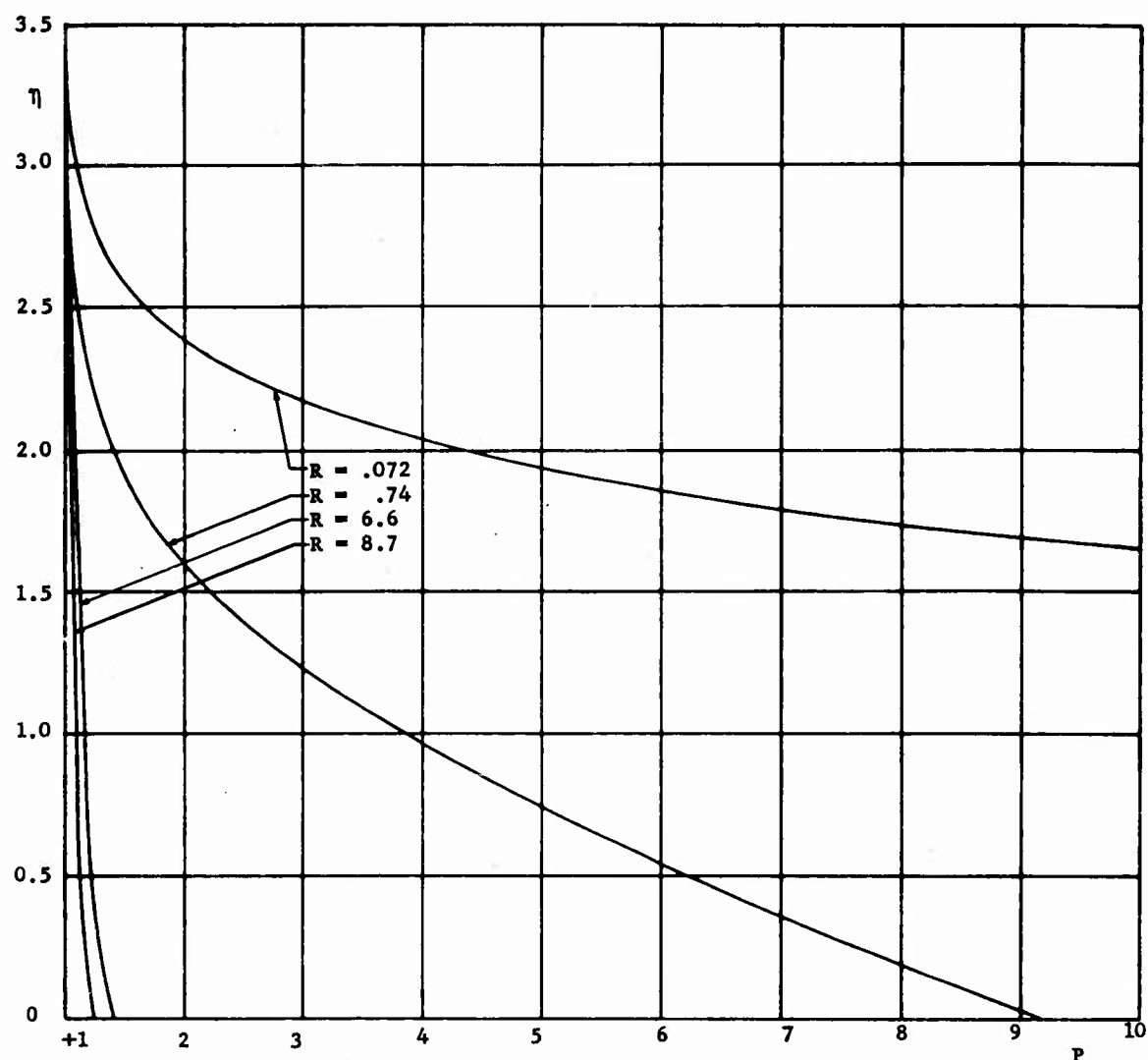
FIGURE 10: The pressure distribution P of axisymmetric wake flows vs. the dimension-
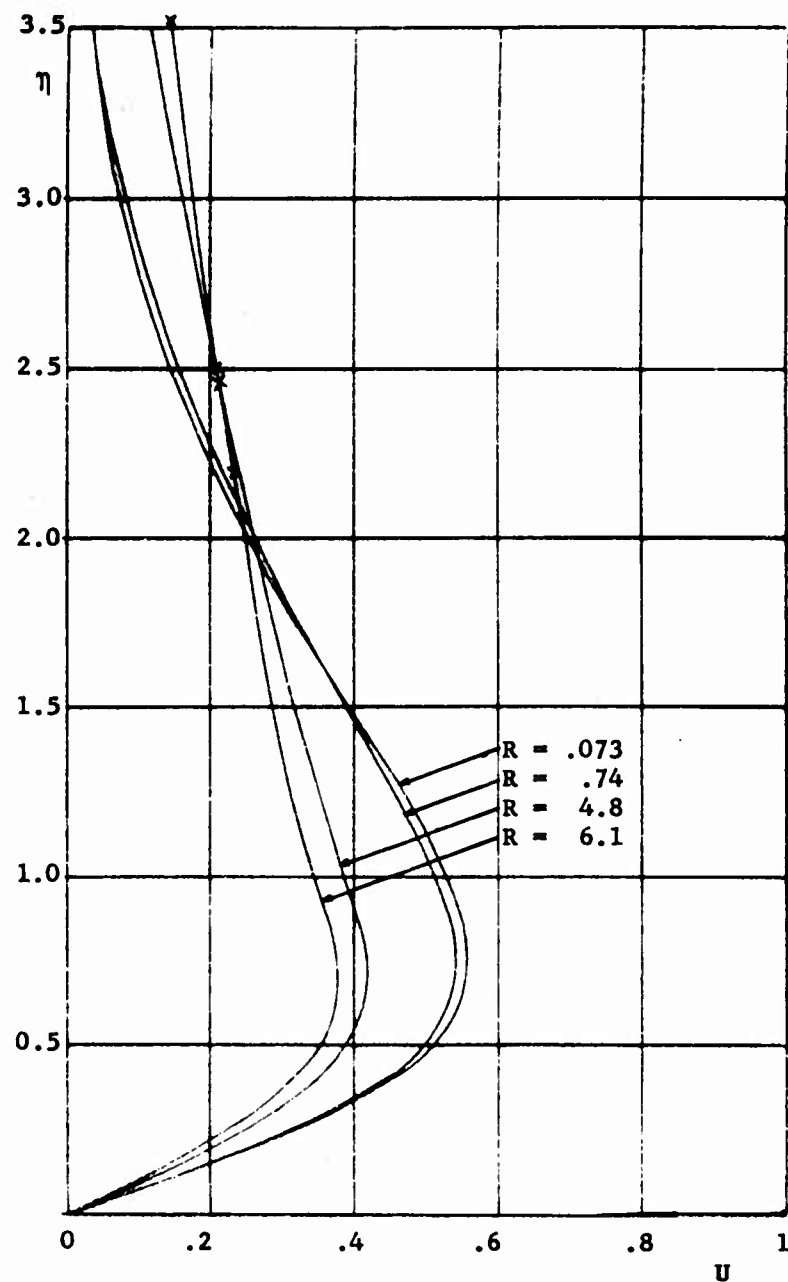less variable η for four different Reynolds numbers R.

FIGURE 11: The horizontal velocity U of plane wake flows vs. the dimensionless variable η for four different Reynolds numbers R. (*Inflection point of instability)
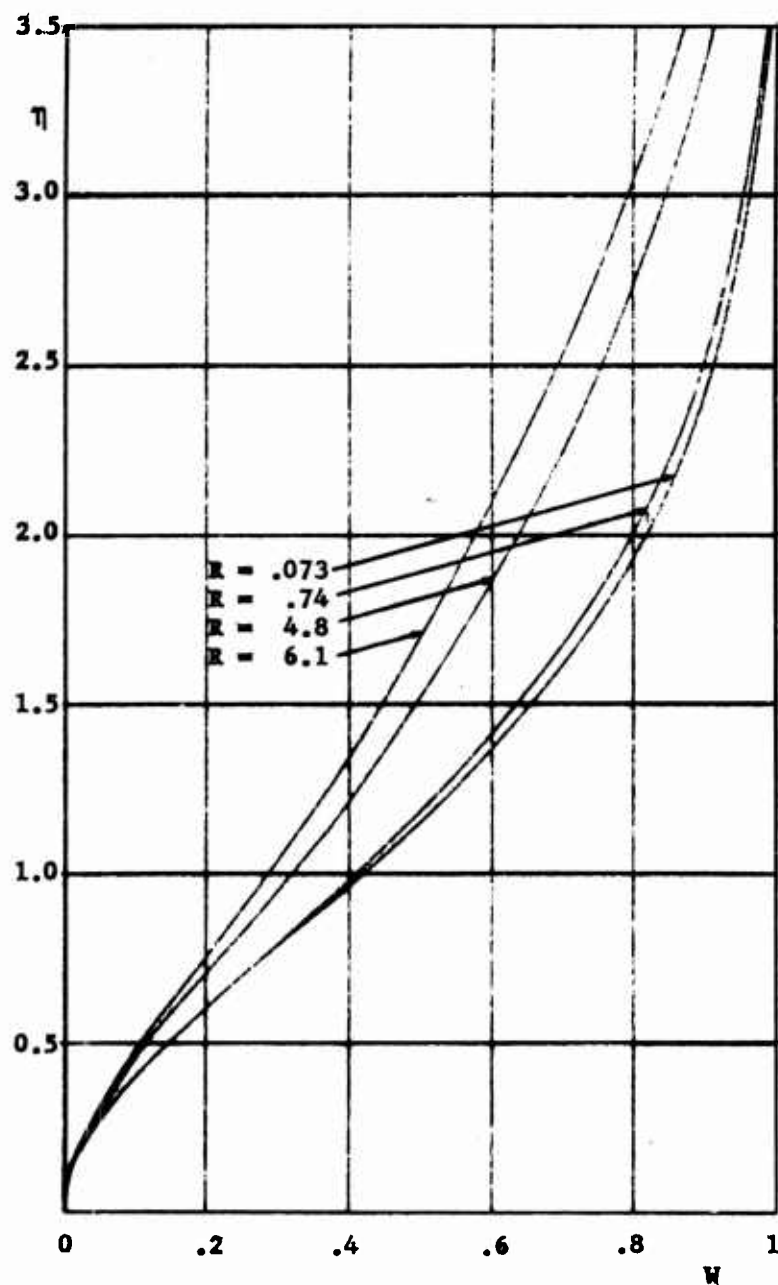
FIGURE 12: The vertical velocity W of plane wake flows vs. the
dimensionless variable η for four different Reynolds
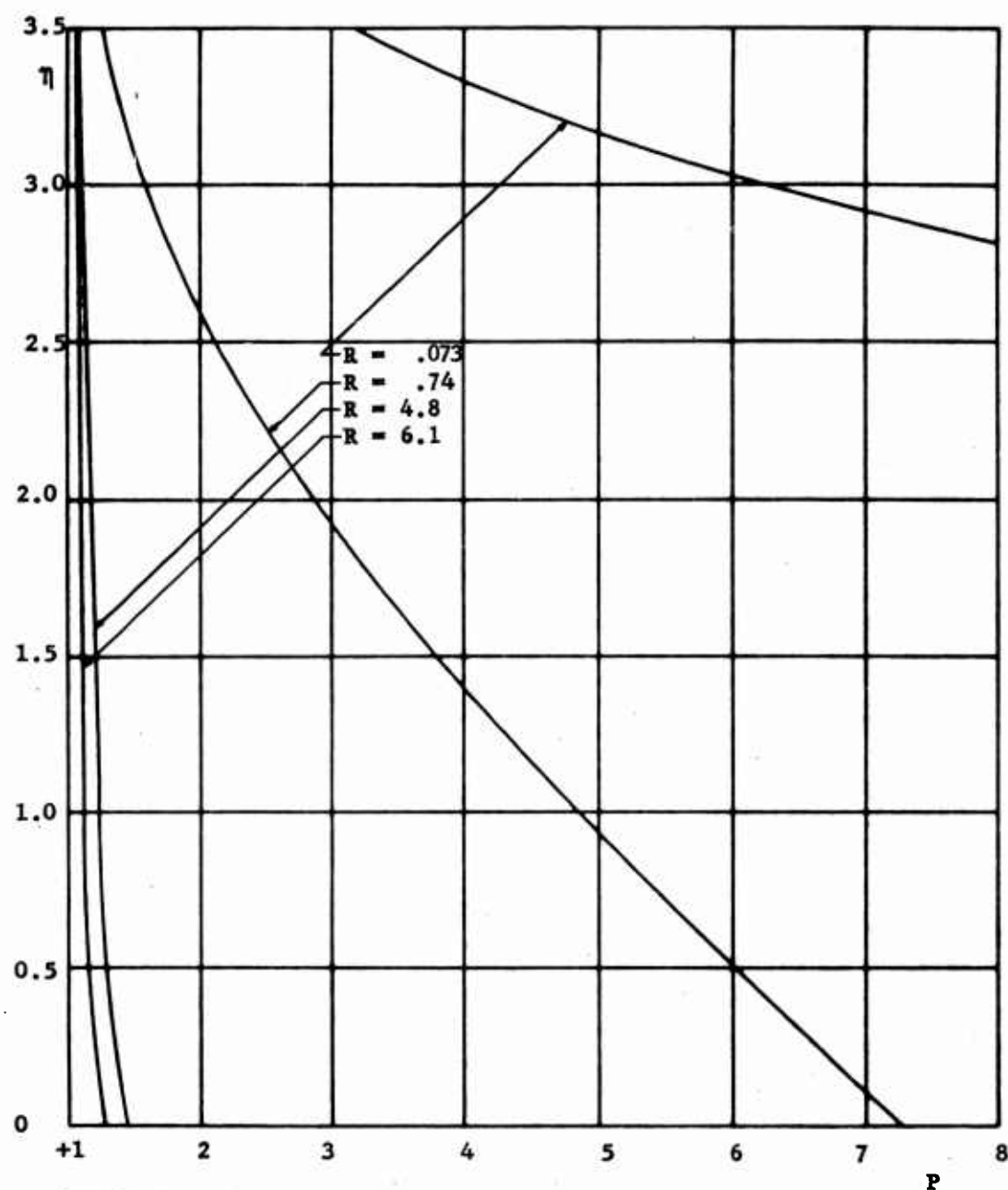numbers R.

FIGURE 13: The pressure distribution P of plane wake flows vs. the dimensionless variable η for four different Reynolds numbers R.
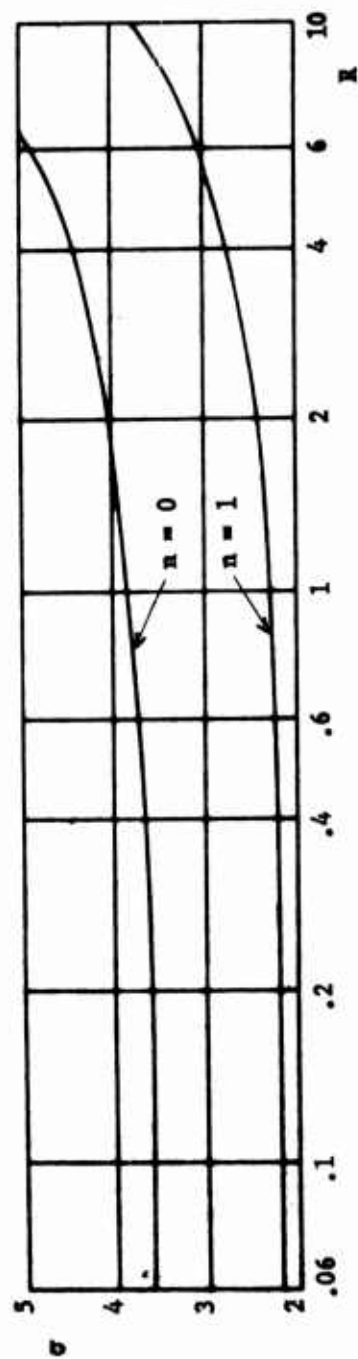
FIGURE 15: The characteristic number σ of axisymmetric (n = 1) and plane (n = 0) wake flows for an accuracy of 1% vs. the Reynolds number R.
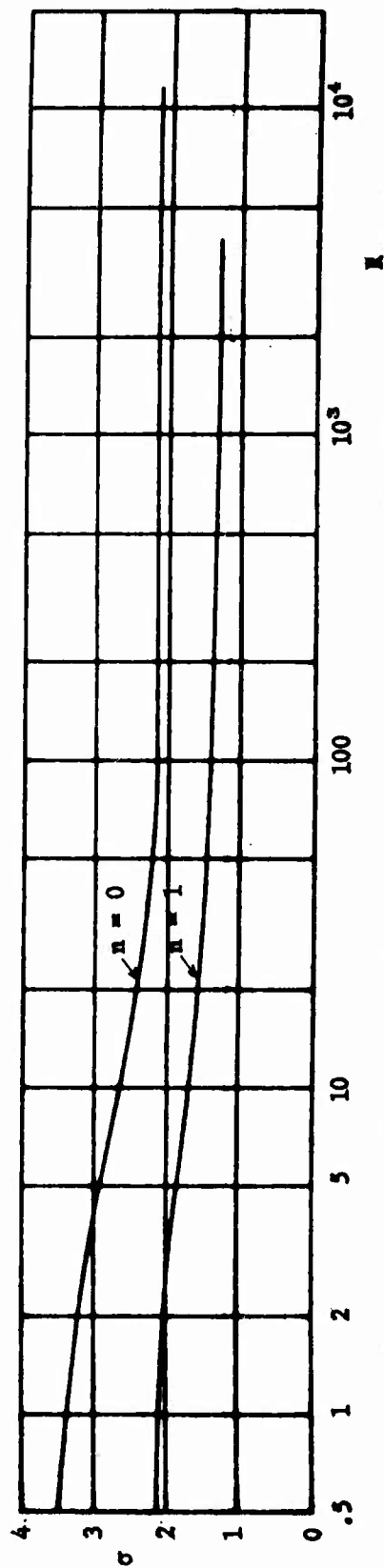

FIGURE 14: The characteristic number σ of axisymmetric (n = 1) and plane (n = 0) stagnation flows for an accuracy of 1% vs. the Reynolds number R.

APPENDIX C

DISTRIBUTION

Bureau of Naval Weapons

DLI-3	1
R-14	1
R-12	1
RREN	1
RRE	1
RT	1
RM	1

Special Projects Office
Department of the Navy
Washington 25, D. C.

SP-20	4
SP-43	2

Commander
Armed Services Technical Information Agency
Arlington Hall Station
Arlington 12, Virginia
    Attn: TIPDR   10

Commanding General
Aberdeen Proving Ground
Aberdeen, Maryland
    Attn: Technical Information Section
           Development and Proof Services   2

Commander, Operational and Development Force
U. S. Atlantic Fleet, U. S. Naval Base
Norfolk 11, Virginia   1

Chief of Naval Research
Department of the Navy
Washington 25, D. C.
    Attn: Code 438   2
    Attn: Mathematical Sciences Division   1
    Attn: Dr. F. J. Weyl   1
    Attn: Mathematics Branch   1
    Attn: Fluid Dynamics Branch   1

DISTRIBUTION (Continued)

Director
Naval Research Laboratory
Washington 25, D. C.   3

Commander
Naval Ordnance Laboratory
White Oak, Maryland
    Attn: Dr. R. Roberts   1
    Attn: Dr. R. E. Wilson   2
    Attn: Dr. A. VanTuyl   1
    Attn: Technical Library   1

Chief, Bureau of Ships
Department of the Navy
Washington 25, D. C.   2

Director
David Taylor Model Basin
Washington 7, D. C.
    Attn: Dr. Daniel Shanks   1
    Attn: Dr. John W. Wrench, Jr.   1
    Attn: Dr. F. D. Murnaghan   1
    Attn: Dr. H. Polachek   1
    Attn: Dr. Elizabeth Cuthill   2
    Attn: Library   2

Commander
U. S. Naval Ordnance Test Station
China Lake, California
    Attn: Dr. D. E. Zilmer   1
    Attn: Library   2

Superintendent
U. S. Naval Postgraduate School
Monterey, California
    Attn: Library, Technical Reports Section   1

Director of the Institute of Naval Studies
185 Alewife Brook Parkway
Cambridge 38, Massachusetts   1

DISTRIBUTION (Continued)

Commanding General
White Sands Proving Ground
La Cruces, New Mexico
    Attn: Flight Determination Laboratory   1

Commander, 3206th Test Group
Building 100
Eglin Air Force Base, Florida
    Attn: Mr. H. L. Adams   1

Commander
Wright Air Development Center
Wright-Patterson Air Force Base
Dayton, Ohio
    Attn: WCRRN-4   1
    Attn: Dr. K. G. Guderley   1

U. S. Atomic Energy Commission
Washington, D. C.
    Attn: Technical Library   1

Los Alamos Scientific Laboratory
Los Alamos, New Mexico   2

Superintendent
U. S. Naval Academy
Annapolis, Maryland
    Attn: Dept. of Mathematics   1
    Attn: Library   1

U. S. Naval Observatory
Washington 25, D. C.
    Attn: Dr. G. M. Clemence   1

U. S. Weather Bureau
Washington 25, D. C.
    Attn: Dr. J. Smagorinsky   1

Commander
Naval Ordnance Test Station
Pasadena Annex
3202 Foothill Boulevard
Pasadena, California   1

DISTRIBUTION (Continued)

Bureau of Naval Weapons Representative P. O. Box 594 Sunnyvale, California Attn: BUWEPSREP-314	1
Army Rocket and Guided Missile Agency U. S. Army Ordnance Missile Command Redstone Arsenal, Alabama Attn: Capt. Robert H. C. Au	1
National Aeronautics and Space Administration 1520 H Street, N. W. Washington 25, D. C.	6
Commander Ballistic Missile Division ARDC P. O. Box 262 Inglewood, California Attn: Col. Ebelke (WDTVR)	2

Commanding General
Army Ballistic Missile Agency
Redstone Arsenal
Huntsville, Alabama
    Attn: Mr. H. G. Paul (ORDAB - DS)   1
    Attn: Dr. W. Lucas (ORDAB - DS)   1
    Attn: Mr. Dale L. Burrows (ORDAB - DSDA)   1
    Attn: Technical Library   1

National Science Foundation
1520 H. Street, N. W.
Washington, D. C.
    Attn: Engineering Sciences Division   1
    Attn: Mathematical Sciences Division   1

Director
National Bureau of Standards
Washington 25, D. C.
    Attn: Fluid Mechanics Division   1
    Attn: Dr. G. B. Schubauer   1
    Attn: Dr. G. H. Keulegan   1
    Attn: Mr. J. H. Wegstein, Computation Laboratory   1
    Attn: Dr. Phillip Davis   1
    Attn: Dr. E. W. Cannon, Applied Mathematics Division   1
    Attn: Dr. S. N. Alexander, Data Processing Division   1
    Attn: Dr. R. J. Arms   1
    Attn: Technical Library   1

DISTRIBUTION (Continued)

Office of Technical Services
Department of Commerce
Washington 25, D. C.   1

Guggenheim Aeronautical Laboratory
California Institute of Technology
Pasadena 4, California
    Attn: Prof. Lester Lees   1
    Attn: Prof. J. D. Cole   1

California Institute of Technology
Pasadena 4, California
    Attn: Prof. John Todd   1

University of California
Berkeley 4, California
    Attn: Department of Mathematics   1

Institute of Mathematical Sciences
New York University
25 Waverly Place
New York 3, New York
    Attn: Prof. K. O. Friedrichs   1
    Attn: Prof. J. J. Stoker   1
    Attn: Dr. Max Goldstein   1
    Attn: Prof. B. Haurwitz   1
    Attn: AEC Computing Facility   1

Harvard University
Cambridge 38, Massachusetts
    Attn: Prof. G. Birkhoff   1
    Attn: Division of Applied Sciences   1
    Attn: Computation Laboratory   1
    Attn: Prof. G. F. Carrier   1
    Attn: Prof. H. M. Stommel   1

University of Maryland
College Park, Maryland
    Attn: Department of Mathematics   1
    Attn: Institute for Fluid Dynamics and Applied
        Mathematics   1

DISTRIBUTION (Continued)

Massachusetts Institute of Technology
Cambridge, Mass.
    Attn: Prof. C. C. Lin   1
    Attn: Prof. A. H. Shapiro   1
    Attn: Prof. J. G. Charney   1

The Johns Hopkins University
Baltimore 18, Maryland
    Attn: Prof. R. R. Long   1

Applied Physics Laboratory
Johns Hopkins University
Silver Spring, Maryland
    Attn: Librarian   2

University of California
San Diego, California
    Attn: Prof. W. H. Munk   1

University of Chicago
Chicago, Illinois
    Attn: Prof. H. Riehl   1

AVCO Manufacturing Corporation
Research and Advanced Development Division
201 Lowell Street
Wilmington, Massachusetts
    Attn: J. P. Wamser
    Via: INSMAT, Boston, Massachusetts   2

General Electric Co.
Missile and Space Vehicle Department
3198 Chestnut Street
Philadelphia 4, Pennsylvania
    Attn: Mr. R. J. Kirby
    Via: INSMAT, Philadelphia, Upper Darby, Pa.   2

Lewis Flight Propulsion Laboratory
National Aeronautics and Space Administration
Cleveland, Ohio
    Attn: F. K. Moore   1
    Attn: S. H. Maslen   1
    Attn: W. E. Moeckel   1

DISTRIBUTION (Continued)

Lockheed Aircraft Corporation
Palo Alto, California
    Attn: Dr. W. C. Griffith   1

Prof. M. Van Dyke
Department of Aeronautical Engineering
Stanford University
Stanford, California   1

Dr. Bernd Zondek
Computer Usage Company, Inc.
18 East 41st Street
New York 17, N. Y.   1

Prof. J. Siekmann
University of Florida
Gainesville, Florida   1

Dr. L. M. Mack
Jet Propulsion Laboratory
California Institute of Technology
Pasadena, California   1

Prof. W. D. Hayes
Department of Aeronautical Engineering
Princeton University
Princeton, N. J.   1

Prof. R. F. Probstein
Division of Engineering
Brown University
Providence 12, R. I.   1

Dr. C. C. Bramble
145 Monticello
Annapolis, Maryland   1

Dr. M. J. Lighthill
Royal Aircraft Establishment
Farnborough, Hampshire, England
Via: BUWEPS (DSC-3)   1

Prof. G. K. Batchelor
University of Cambridge
Cambridge, England
Via: BUWEPS (DSC-3)   1

DISTRIBUTION (Continued)

Prof. C. R. Illingworth University of Manchester Manchester, England Via: BUWEPS (DSC-3)	1
Prof. Dr. H. Goertler University of Freiburg Freiburg, Germany Via: BUWEPS (DSC-3)	1
Prof. Dr. H. Schlichting Technische Hochschule Braunschweig, Germany Via: BUWEPS (DSC-3)	1
Prof. Dr. W. Tollmien Max Planck Institute Goettingen, Germany Via: BUWEPS (DSC-3)	1
Prof. Dr. A. Naumann Technische Hochschule Aachen Aachen, Germany Via: BUWEPS (DSC-3)	1
Prof. Dr. J. Ackeret Eidgenoessische Technische Hochschule Zurich, Switzerland Via: BUWEPS (DSC-3)	1

Local:

D	1
K	1
K-1	1
K-3	1
K-4	1
KXK	1
KXF	1
KXH	1
KYD	2
KXL	25
KYS	50
ACL	5
File	1

LIBRARY CATALOGING INPUT
PRNC-NWL-5070/15 (7-62)

BIBLIOGRAPHIC INFORMATION

DESCRIPTOR	CODE	DESCRIPTOR	CODE
SOURCE NWL Report	NPGA	**SECURITY CLASSIFICATION AND CODE COUNT** UNCLASSIFIED	UO18
REPORT NUMBER 1840	1840	**CIRCULATION LIMITATION**	
REPORT DATE February 1963	0263	**CIRCULATION LIMITATION OR BIBLIOGRAPHIC**	
		BIBLIOGRAPHIC (Suppl., Vol., etc.)	

SUBJECT ANALYSIS OF REPORT

DESCRIPTOR	CODE	DESCRIPTOR	CODE	DESCRIPTOR	CODE
Stagnation	STAG	Differential	DIFE		
Wakes	WAKE	Equations	EQUA		
Flow	FLOW	Reynolds number	REYN		
Normal (Mathematics)	NORM	Plane	PLNE		
Flat	FLAT				
Surfaces	SURA				
Properties	PROP				
Axial	AXIA				
Symmetrical	SYMM				
Prandtl	PRAN				
Boundary layer	BOUL				
Theory	THEY				
Navier-Stokes	NAVE				
Partial	PARI				

Naval Weapons Laboratory, Dahlgren, Virginia.
(NWL Report No. 1840)
STAGNATION AND WAKE FLOWS NORMAL TO A FLAT
SURFACE, by E. W. Schwiderski and H. J. Lugt.
Feb 1963. 12 p., 15 figs., 12 tables.
UNCLASSIFIED

Numerical results of axisymmetric and
plane stagnation and wake flows normal to a
flat surface are presented for various
Reynolds numbers. Characteristic flow
properties are discussed. Critical Reynolds
numbers for nonexistent laminar attached
flows are computed.

1. Boundary layer -
   Theory
2. Meteorology
3. Vortex reactor
4. Partial differential
   equations
I. Schwiderski, E. W.
II. Lugt, H. J.

Task: R360FR103/2101/
R01101001

UNCLASSIFIED

Naval Weapons Laboratory, Dahlgren, Virginia.
(NWL Report No. 1840)
STAGNATION AND WAKE FLOWS NORMAL TO A FLAT
SURFACE, by E. W. Schwiderski and H. J. Lugt.
Feb 1963. 12 p., 15 figs., 12 tables.
UNCLASSIFIED

Numerical results of axisymmetric and
plane stagnation and wake flows normal to a
flat surface are presented for various
Reynolds numbers. Characteristic flow
properties are discussed. Critical Reynolds
numbers for nonexistent laminar attached
flows are computed.

1. Boundary layer -
   Theory
2. Meteorology
3. Vortex reactor
4. Partial differential
   equations
I. Schwiderski, E. W.
II. Lugt, H. J.

Task: R360FR103/2101/
R01101001

UNCLASSIFIED

Naval Weapons Laboratory, Dahlgren, Virginia.
(NWL Report No. 1840)
STAGNATION AND WAKE FLOWS NORMAL TO A FLAT
SURFACE, by E. W. Schwiderski and H. J. Lugt.
Feb 1963. 12 p., 15 figs., 12 tables.
UNCLASSIFIED

Numerical results of axisymmetric and
plane stagnation and wake flows normal to a
flat surface are presented for various
Reynolds numbers. Characteristic flow
properties are discussed. Critical Reynolds
numbers for nonexistent laminar attached
flows are computed.

1. Boundary layer -
   Theory
2. Meteorology
3. Vortex reactor
4. Partial differential
   equations
I. Schwiderski, E. W.
II. Lugt, H. J.

Task: R360FR103/2101/
R01101001

UNCLASSIFIED

Naval Weapons Laboratory, Dahlgren, Virginia.
(NWL Report No. 1840)
STAGNATION AND WAKE FLOWS NORMAL TO A FLAT
SURFACE, by E. W. Schwiderski and H. J. Lugt.
Feb 1963. 12 p., 15 figs., 12 tables.
UNCLASSIFIED

Numerical results of axisymmetric and
plane stagnation and wake flows normal to a
flat surface are presented for various
Reynolds numbers. Characteristic flow
properties are discussed. Critical Reynolds
numbers for nonexistent laminar attached
flows are computed.

1. Boundary layer -
   Theory
2. Meteorology
3. Vortex reactor
4. Partial differential
   equations
I. Schwiderski, E. W.
II. Lugt, H. J.

Task: R360FR103/2101/
R01101001

UNCLASSIFIED

Naval Weapons Laboratory, Dahlgren, Virginia.
(NWL Report No. 1840)
STAGNATION AND WAKE FLOWS NORMAL TO A FLAT
SURFACE, by E. W. Schwiderski and H. J. Lugt.
Feb 1963. 12 p., 15 figs., 12 tables.
UNCLASSIFIED

Numerical results of axisymmetric and
plane stagnation and wake flows normal to a
flat surface are presented for various
Reynolds numbers. Characteristic flow
properties are discussed. Critical Reynolds
numbers for nonexistent laminar attached
flows are computed.

1. Boundary layer -
   Theory
2. Meteorology
3. Vortex reactor
4. Partial differential
   equations
I. Schwiderski, E. W.
II. Lugt, H. J.

Task: R360FR103/2101/
R01101001

UNCLASSIFIED

Naval Weapons Laboratory, Dahlgren, Virginia.
(NWL Report No. 1840)
STAGNATION AND WAKE FLOWS NORMAL TO A FLAT
SURFACE, by E. W. Schwiderski and H. J. Lugt.
Feb 1963. 12 p., 15 figs., 12 tables.
UNCLASSIFIED

Numerical results of axisymmetric and
plane stagnation and wake flows normal to a
flat surface are presented for various
Reynolds numbers. Characteristic flow
properties are discussed. Critical Reynolds
numbers for nonexistent laminar attached
flows are computed.

1. Boundary layer -
   Theory
2. Meteorology
3. Vortex reactor
4. Partial differential
   equations
I. Schwiderski, E. W.
II. Lugt, H. J.

Task: R360FR103/2101/
R01101001

UNCLASSIFIED

Naval Weapons Laboratory, Dahlgren, Virginia.
(NWL Report No. 1840)
STAGNATION AND WAKE FLOWS NORMAL TO A FLAT
SURFACE, by E. W. Schwiderski and H. J. Lugt.
Feb 1963. 12 p., 15 figs., 12 tables.
UNCLASSIFIED

Numerical results of axisymmetric and
plane stagnation and wake flows normal to a
flat surface are presented for various
Reynolds numbers. Characteristic flow
properties are discussed. Critical Reynolds
numbers for nonexistent laminar attached
flows are computed.

1. Boundary layer -
   Theory
2. Meteorology
3. Vortex reactor
4. Partial differential
   equations
I. Schwiderski, E. W.
II. Lugt, H. J.

Task: R360FR103/2101/
R01101001

UNCLASSIFIED

Naval Weapons Laboratory, Dahlgren, Virginia.
(NWL Report No. 1840)
STAGNATION AND WAKE FLOWS NORMAL TO A FLAT
SURFACE, by E. W. Schwiderski and H. J. Lugt.
Feb 1963. 12 p., 15 figs., 12 tables.
UNCLASSIFIED

Numerical results of axisymmetric and
plane stagnation and wake flows normal to a
flat surface are presented for various
Reynolds numbers. Characteristic flow
properties are discussed. Critical Reynolds
numbers for nonexistent laminar attached
flows are computed.

1. Boundary layer -
   Theory
2. Meteorology
3. Vortex reactor
4. Partial differential
   equations
I. Schwiderski, E. W.
II. Lugt, H. J.

Task: R360FR103/2101/
R01101001

UNCLASSIFIED